Unlocking the Secrets of the Rocky Planets

John Baumgardner

South flank of Bonneville crater, Mars, as viewed by Spirit Rover, day 53.

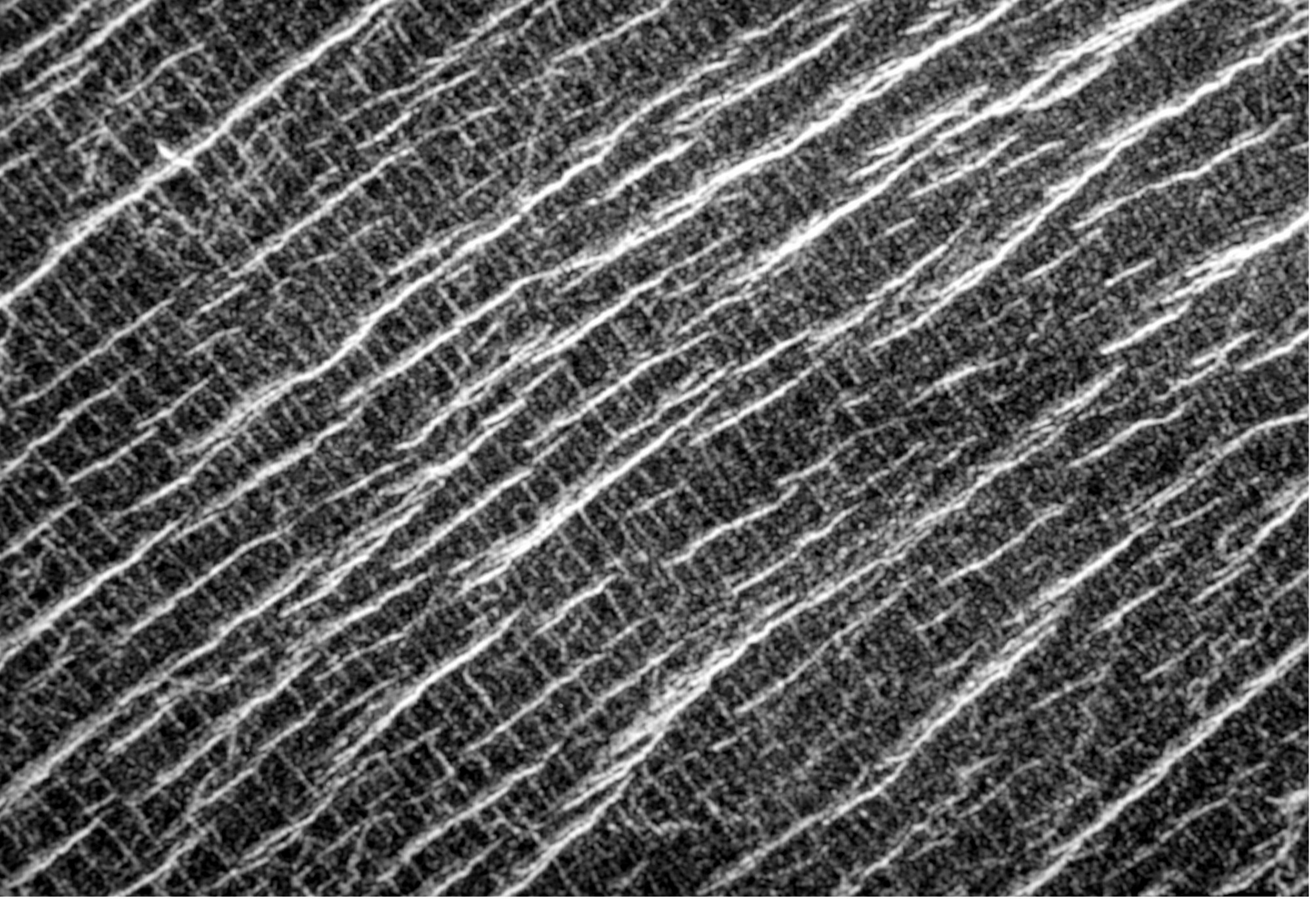

Gridded plains, Venus

Impact crater, Venus

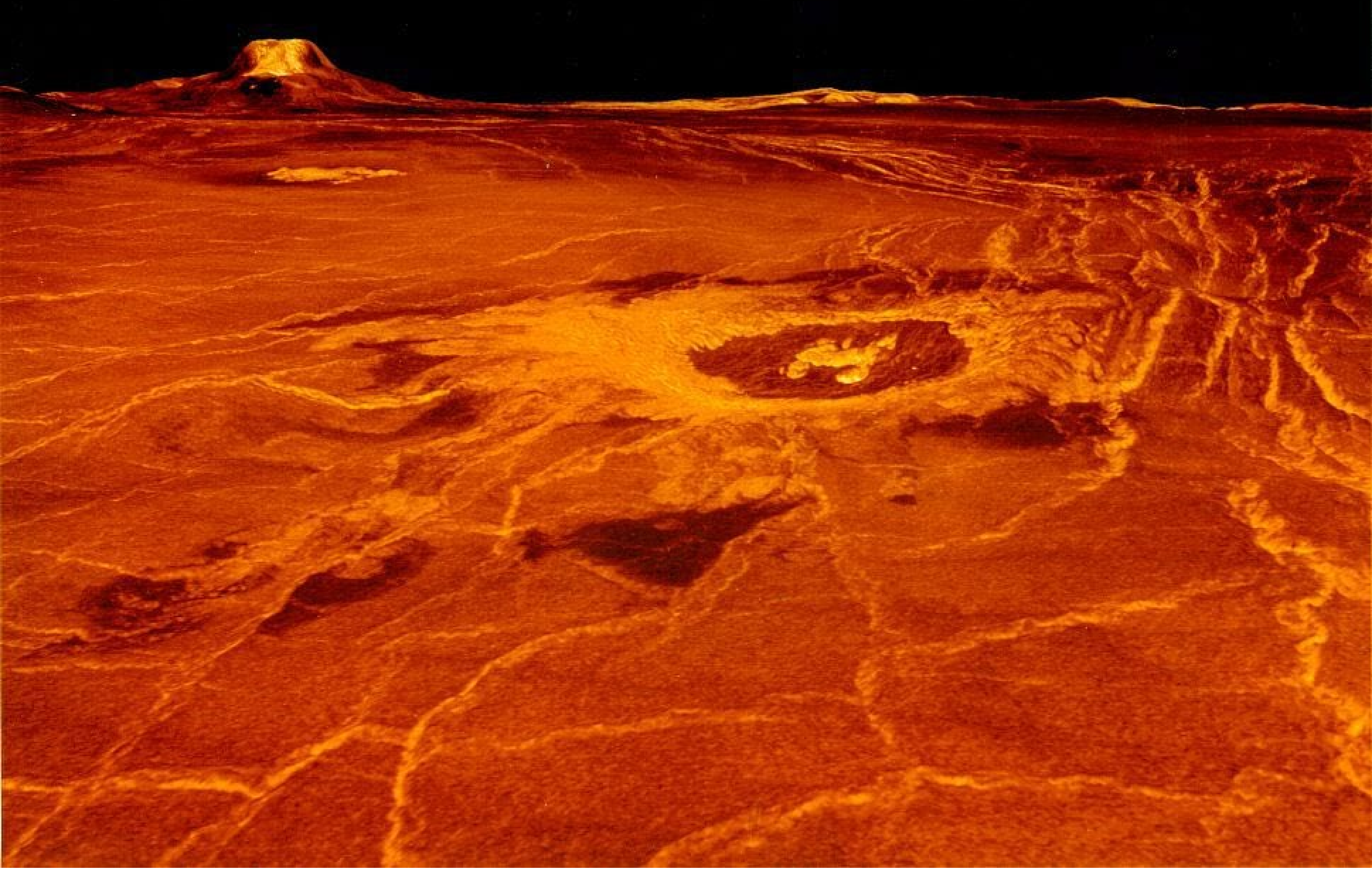

Computer generated surface view, from the southwest, of Eistla Regio of Venus, at 22.5x vertical exaggeration. Gula Mons, the volcano on the left horizon, is 3000 m high and located near 22° latitude and 0° longitude.

Earth from Apollo 16

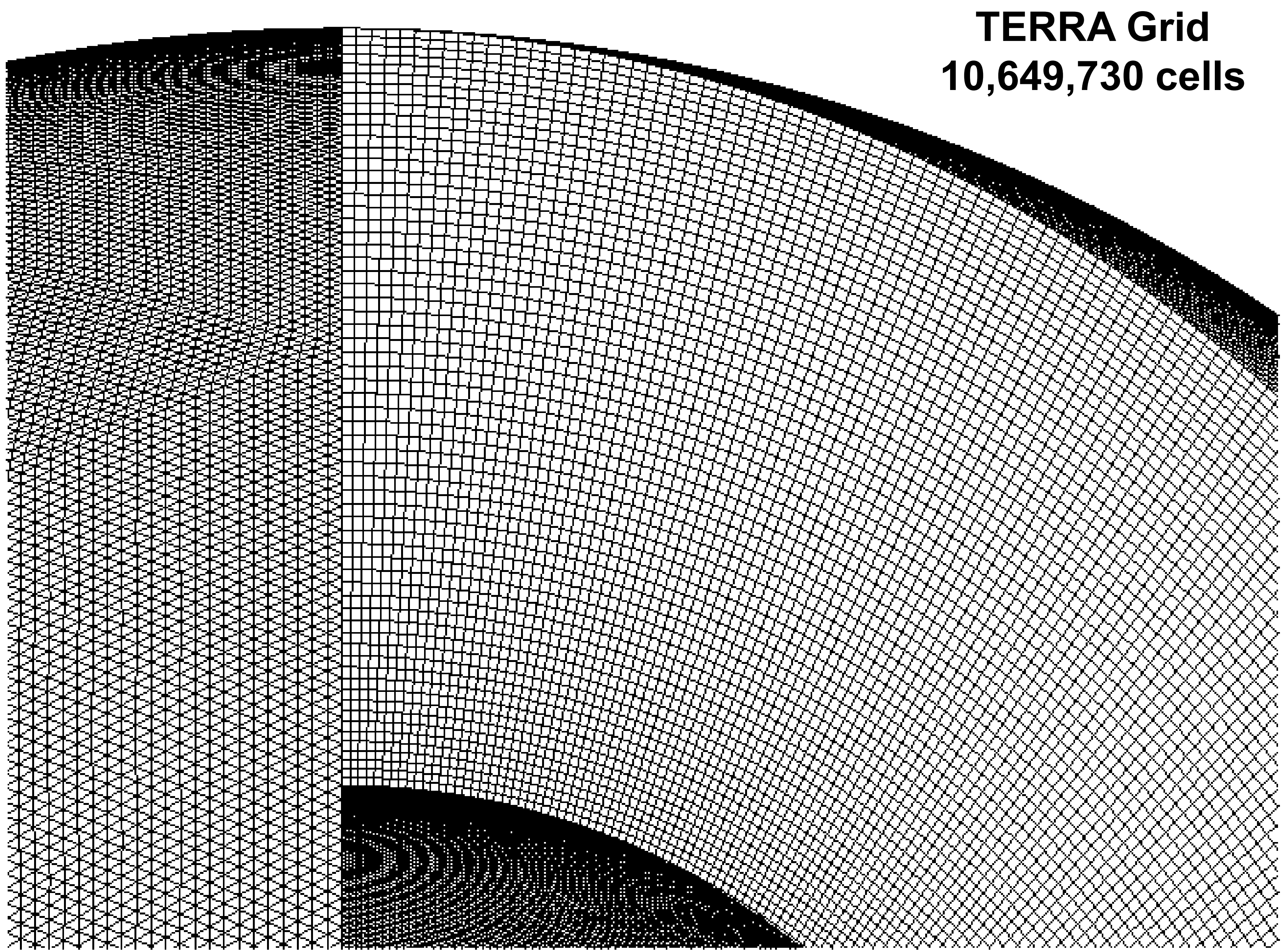
TERRA Grid
10,649,730 cells

Overview of TERRA

- Finite-element formulation (piecewise linear hexagonal prism elements).
- Almost uniform spherical mesh derived from regular icosahedron.
- Regular block data structure naturally suited to domain decomposition.
- Flexibility to treat compressible flow, spatially-varying material properties, real equations of state, and lithospheric plates.

GEODESIC GRIDS CONSTRUCTED FROM THE ICOSAHEDRON

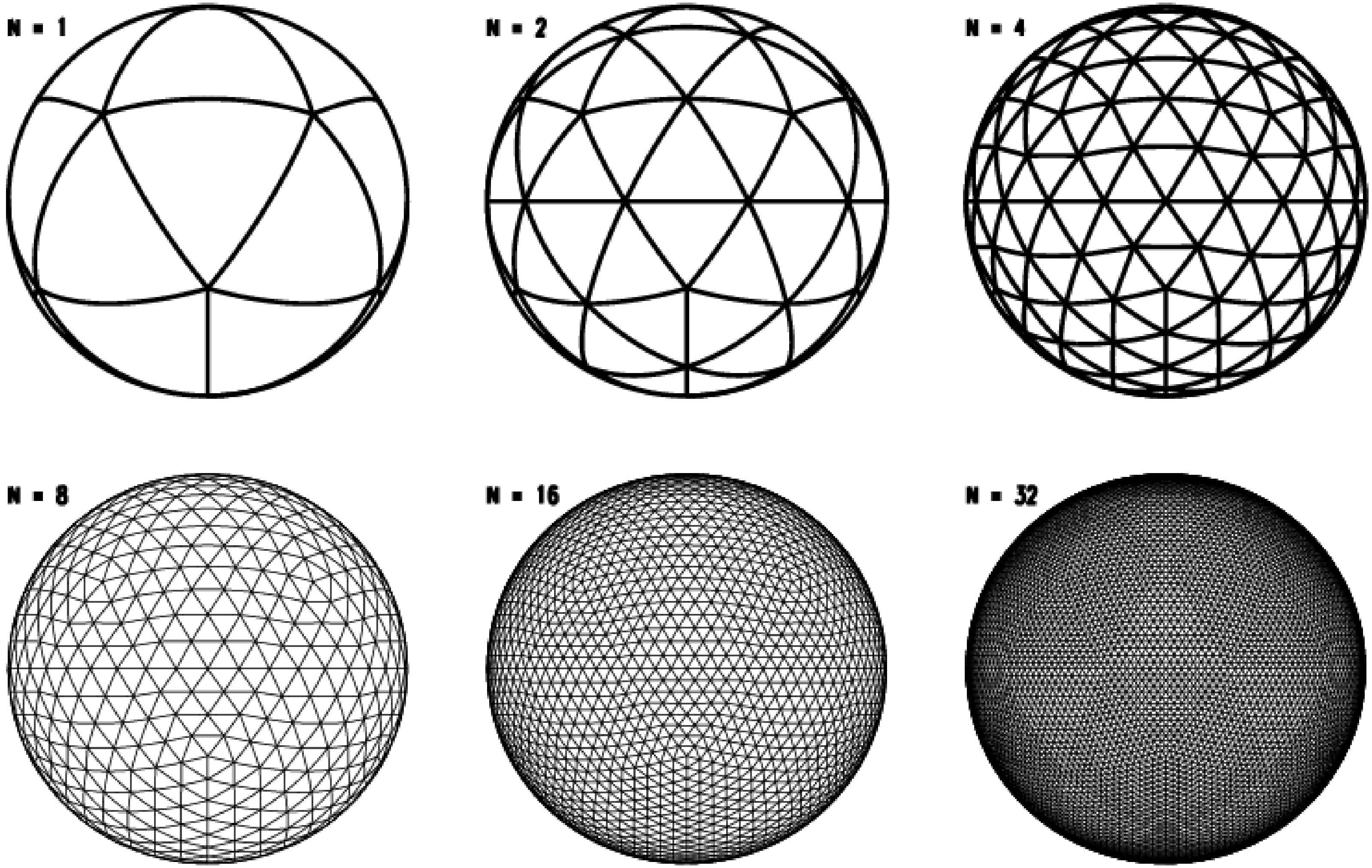

The coarsest grid is constructed by projecting the regular icosahedron onto the sphere to divide its surface into 20 equal spherical triangles. Successively finer grids are obtained by connecting the midpoints of triangle sides with great circle arcs. N is the number of subdivisions of the triangle sides of the coarsest grid.

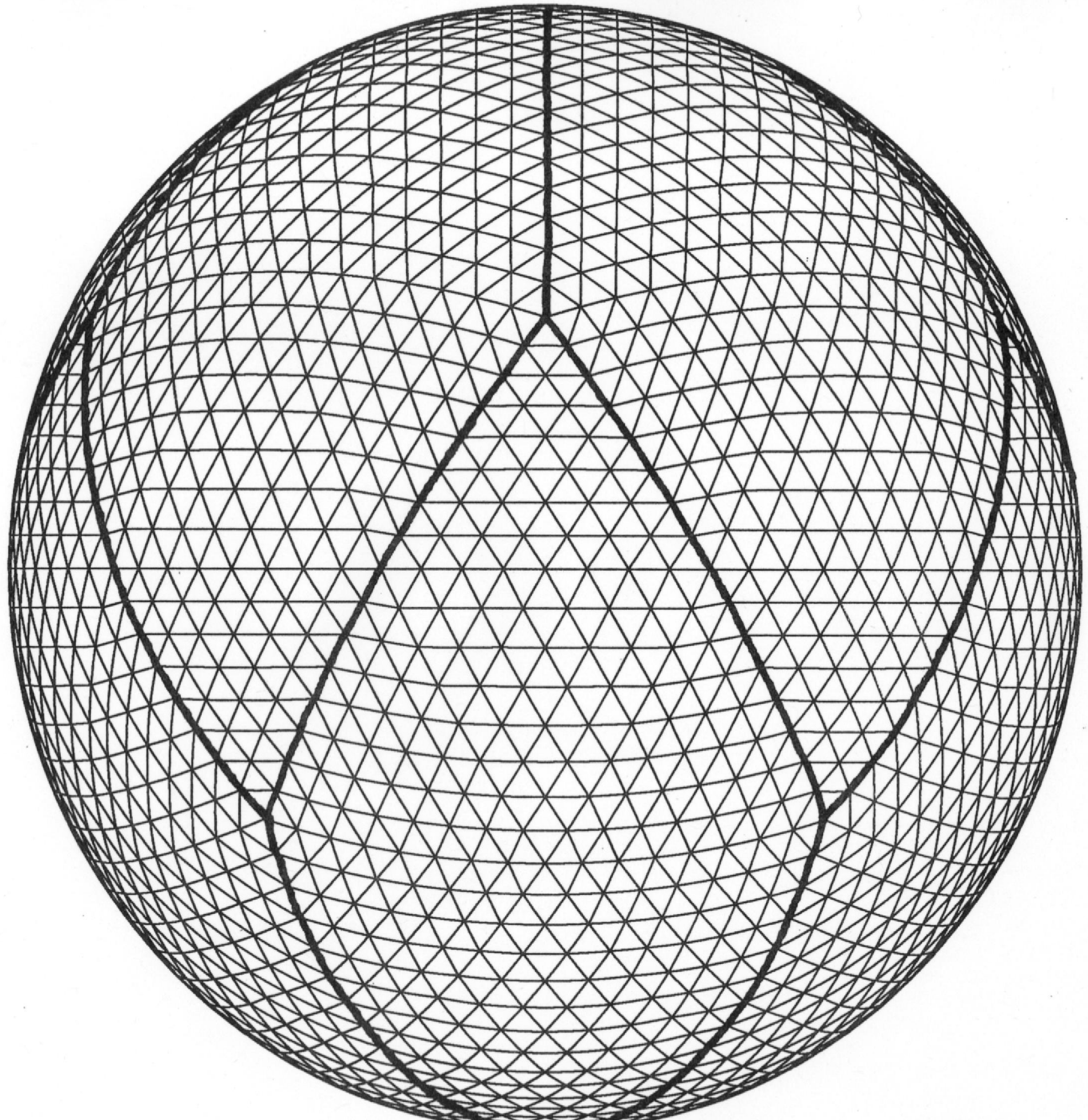

Grid divides into 10 equal logically square subdomains.

Conservation Equations

$$0 = -\nabla(P - P_0) + (\rho - \rho_0)g + \nabla \bullet \underline{\underline{\tau}}$$

$$0 = \nabla \bullet (\rho \underline{u})$$

$$\frac{\partial T}{\partial t} = -\nabla \bullet (T\underline{u}) - (\gamma - 1)T\nabla \bullet \underline{u} + \frac{\nabla \bullet (k\nabla T) + \underline{\underline{\tau}}:\nabla \underline{u} + H}{\rho c_v}$$

where $\quad \underline{\underline{\tau}} = \mu[\nabla \underline{u} + (\nabla \underline{u})^T - \frac{2}{3}\underline{\underline{I}}(\nabla \bullet \underline{u})]$

and $\quad \rho = \rho_0 + \frac{\rho_0 (P - P_0)}{K} - \alpha(T - T_0)$

Features of Multigrid Technique

- Correction method, with line Jacobi smoothing only on the upward part of the (saw-tooth) cycle.
- Matrix-dependent intergrid transfers using the Galerkin coarse grid approximation to handle strong variations in material properties.
- We use a conjugate gradient method (Atanga and Silvester, 1992) as an outer loop to solve for pressure.
- Our algorithms are described in W.-S. Yang and J. R. Baumgardner, "A matrix-dependent transfer multigrid method for strongly variable viscosity infinite Prandtl number thermal convection," *Geophys. Astrophys. Fluid Dynamics*, 92, 151-195, 2000.

The Central Role of Silicate Rheology

The realism of the model depends critically on treating the deformation properties of silicate rock accurately. Strength of silicate minerals depends strongly on temperature and stress.

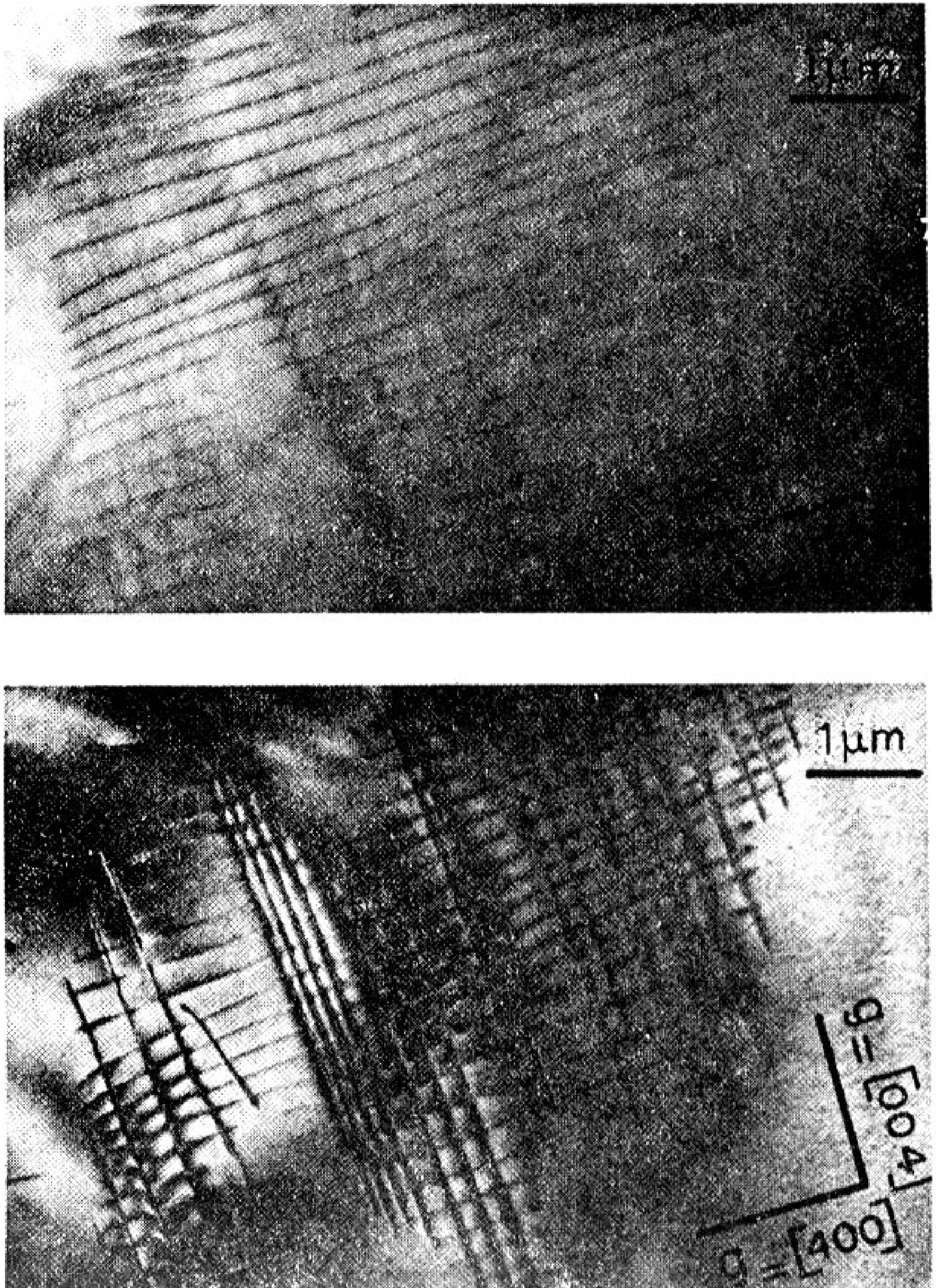

Electron micrograph of dislocation creep deformation in olivine.

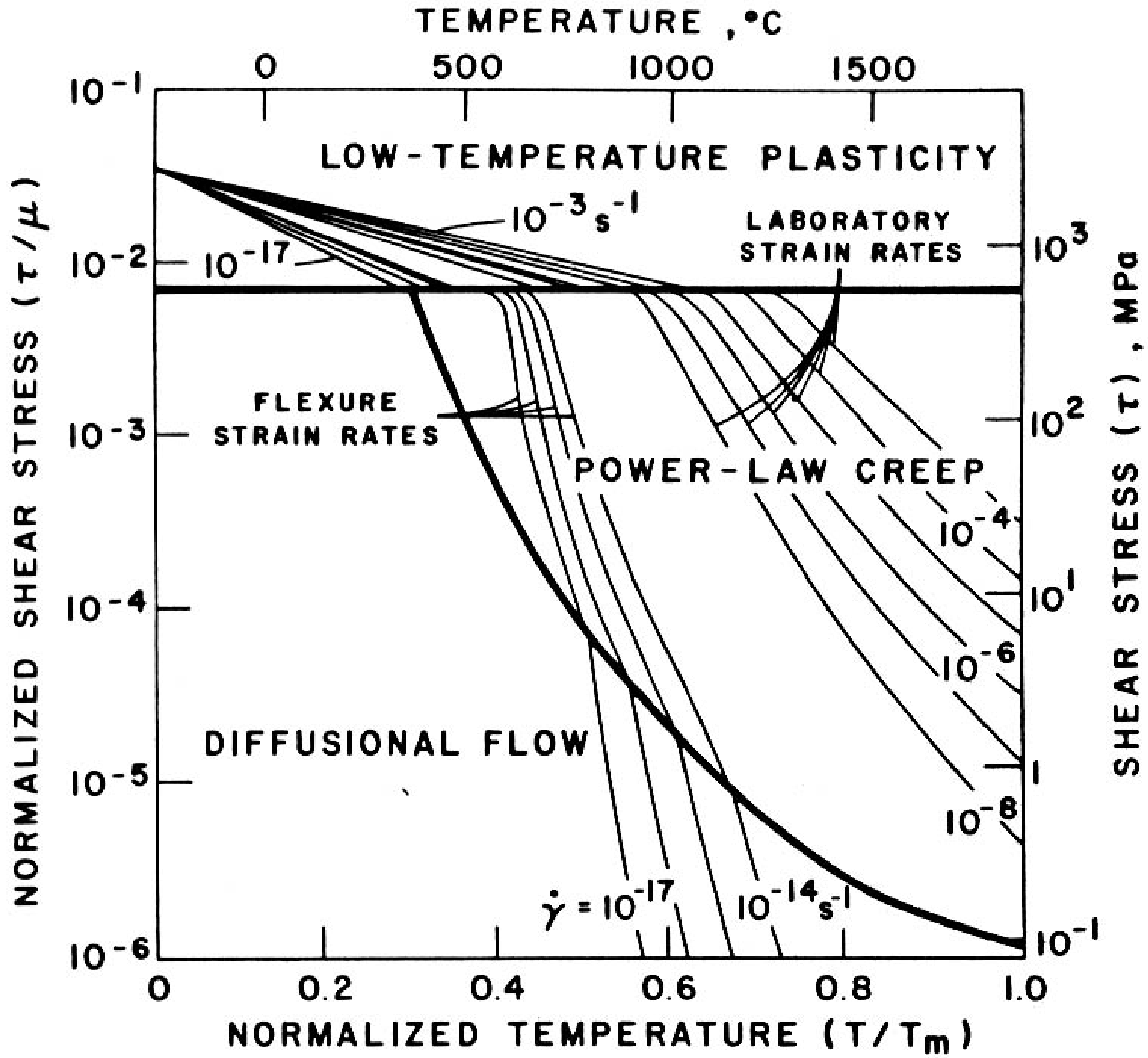

Fig. 1. Deformation mechanism map for olivine with a 1 mm grain size. Shear strain rates $\dot{\gamma}$ (in s^{-1}) are contoured over shear stress τ normalized by shear modulus μ and absolute temperature T normalized by temperature of melting T_m.

Map of the deformational behavior of the mineral olivine, $(Mg,Fe)_2SiO_4$ as a function of temperature and stress.

Some insights provided by TERRA

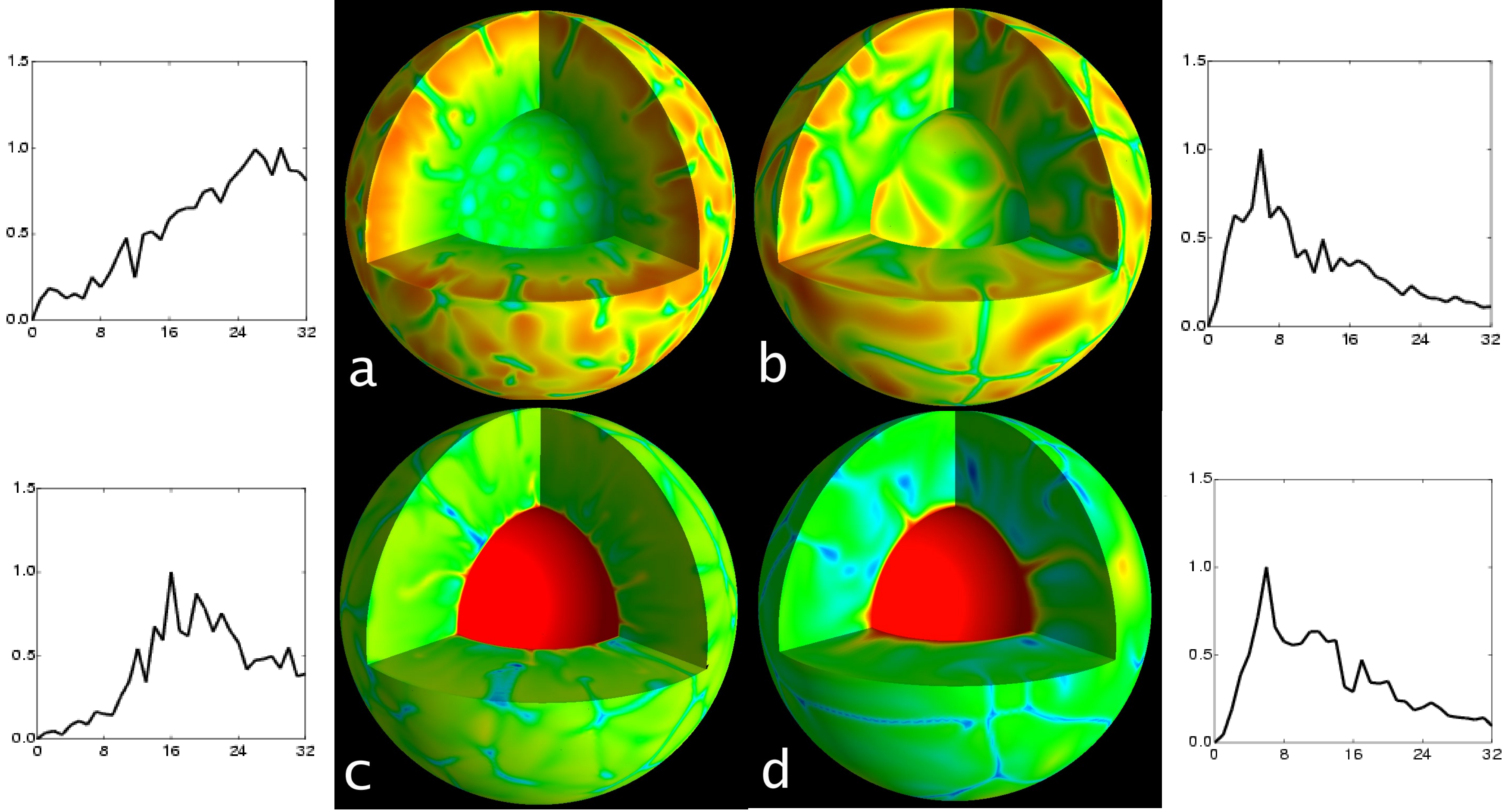

Temperature fields for convection in a spherical shell with geometry of the Earth's mantle. In (a) and (b), the inner boundary is insulating, while in (c) and (d) the inner boundary has a fixed uniform temperature such that about 35% of the total heating is from heat conducted through this lower boundary. The shell has a uniform viscosity in (a) and (c), while in (b) and (d), viscosity increases by a factor of 30 below 700 km. Point-like downwellings characterize the uniform viscosity case, but linear sheet-like downwellings emerge in the case with stratified viscosity. Simply making the lower mantle more viscous, as supported by many lines of observational evidence for the Earth, results in this strikingly more Earth-like pattern of linear downwellings near the surface that correlate with observed subduction at plate edges.

Three-Dimensional Spherical Simulations of Earth's Core and Mantle Dynamics

Peter Olson, Johns Hopkins University, PI
http://www.jhu.edu/~eps/geoplab/nasa3/start.html

TERRA offers a powerful simulation capability to apply the vast datasets from surface geology to constrain and test models of a planet's internal dynamics and history, i.e., advance tangibly the emerging synthesis of geology and geophysics.

Goal: *Simulate the chaotic processes that drive the evolution of the planet's interior, and in turn shape its surface geological features and history.*

TERRA is a 3D spherical finite element mantle dynamics code, developed by John Baumgardner, LANL, and his collaborators.

TERRA treats the silicate rock of the Earth's mantle as a non-linear viscous fluid and solves the Navier-Stokes equations for the motions that arise from variations in temperature and density.

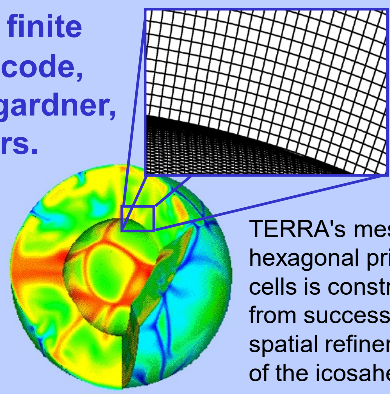

TERRA's mesh of hexagonal prism cells is constructed from successive spatial refinements of the icosahedron.

- Achieved, in Round-2, major algorithmic advances to enable TERRA to treat extreme local variations in material properties.
- Increased the speed of TERRA by a factor of 125.
- Applied TERRA to several fundamental science questions concerning the history and dynamics of the Earth.

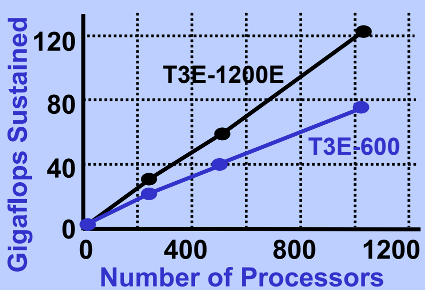

TERRA sustained 121 Gigaflops on 1024 processors of a CRAY T3E-1200E, and 10 Gigaflops on 128 processors of a 350Mhz Pentium-II Linux cluster.

Prior to ESS support, TERRA was baselined in 1995 at 0.96 Gigaflops on a Cray T3D.

The new ability to obtain platelike behavior directly from silicate rheology has opened the door to new discoveries about the Earth's interior

Rheology has to do with material deformation properties.

Recent TERRA simulations confirm that the asthenosphere, a low viscosity zone just below the plates in the Earth, plays a crucial role in stabilizing a plate tectonics style of mantle dynamics.

Required ~5x10^15 floating point operations.

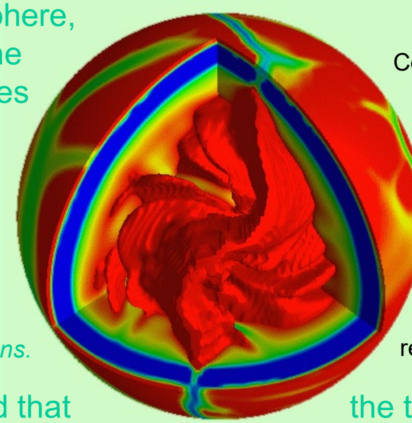

Colors represent viscosity, increasing from blue to red. Note high viscosity surface layer overlying low viscosity asthenosphere. The red isosurface represents cold high viscosity plate material from the surface that is sinking into the deeper mantle. The grid for this case has 10,649,730 cells and a spatial resolution of about 50 km.

TERRA discovered that the tectosphere, a keel-like feature beneath much of the continental area, plays only a very small role in the overall motions of the tectonic plates.

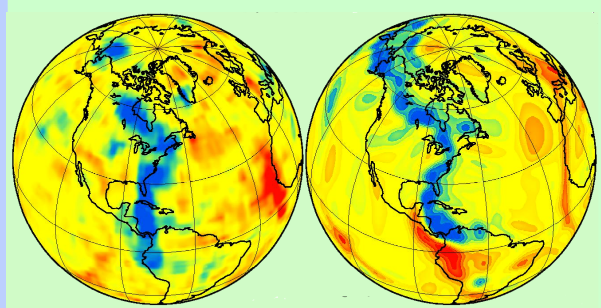

Plot on left is seismic image of Farallon slab (blue). Right plot shows (blue) subducted material in a TERRA simulation based on plate motion history applied as a surface boundary condition.

TERRA demonstrated for the first time the combination of 3D seismic tomography models and 3D geodynamic modeling could improve the accuracy of the plate motion models, here illustrated for the subducted Farallon slab beneath North America.

J.Fischer 010330 (all JPEG?)

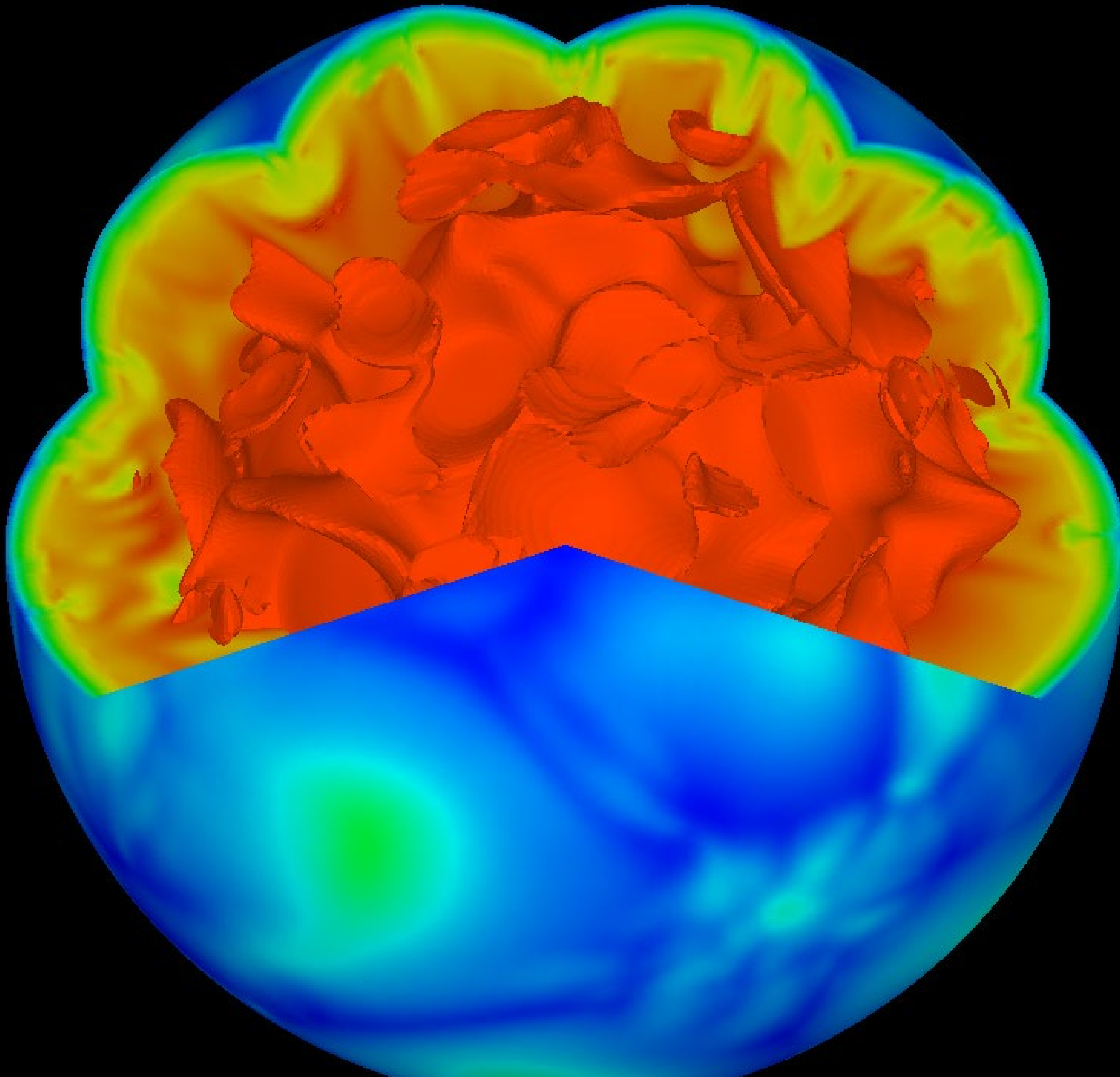

Snapshot of temperature field from isoviscous, internally heated case with Earth mantle geometry.

Note point-like down-wellings from cold upper boundary layer.

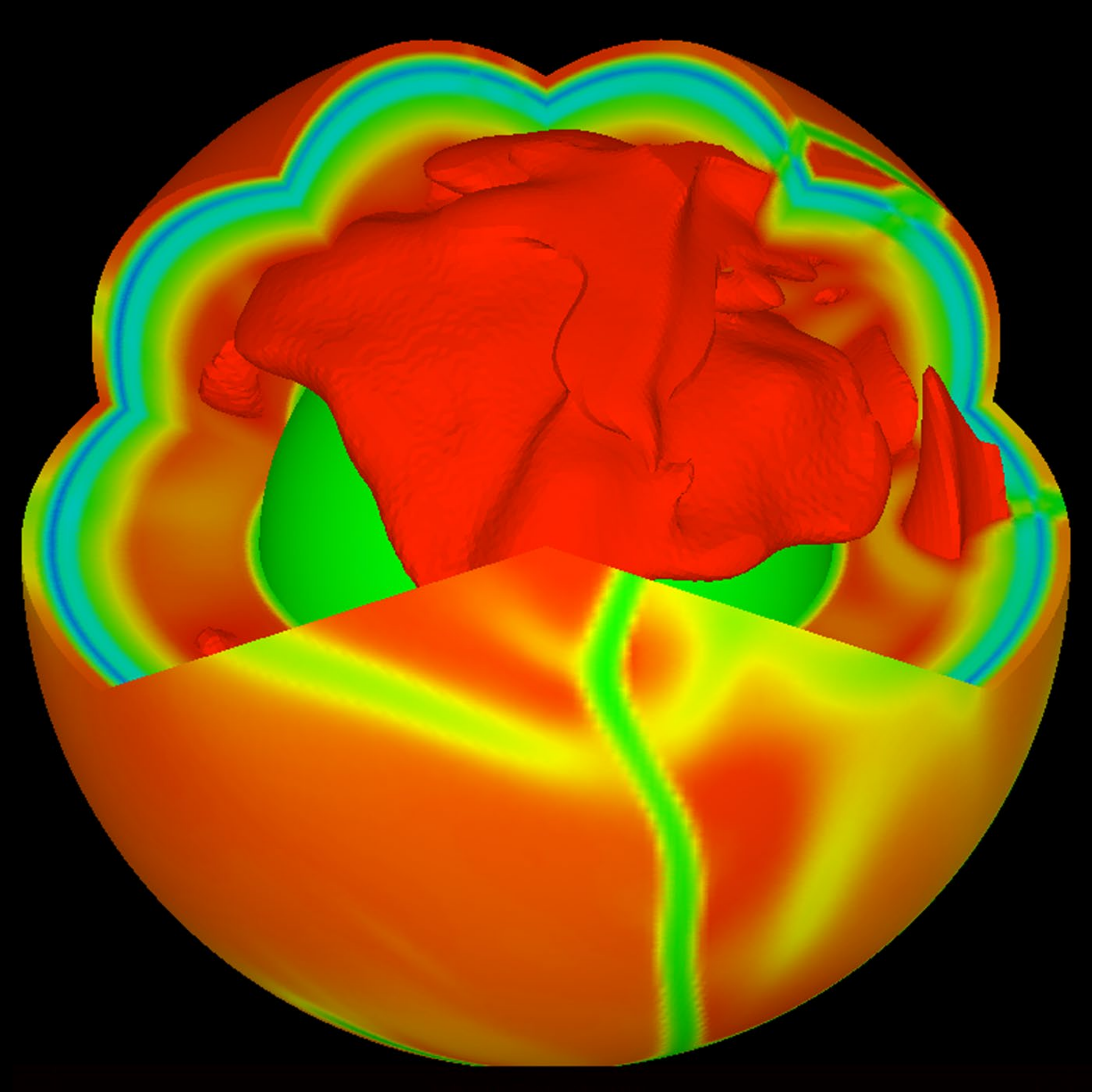

Snapshot from a case with temperature- and stress-dependent rheology.

Downwellings are sheetlike and relatively stable in time.

Surface velocity is beginning to display plate-like character.

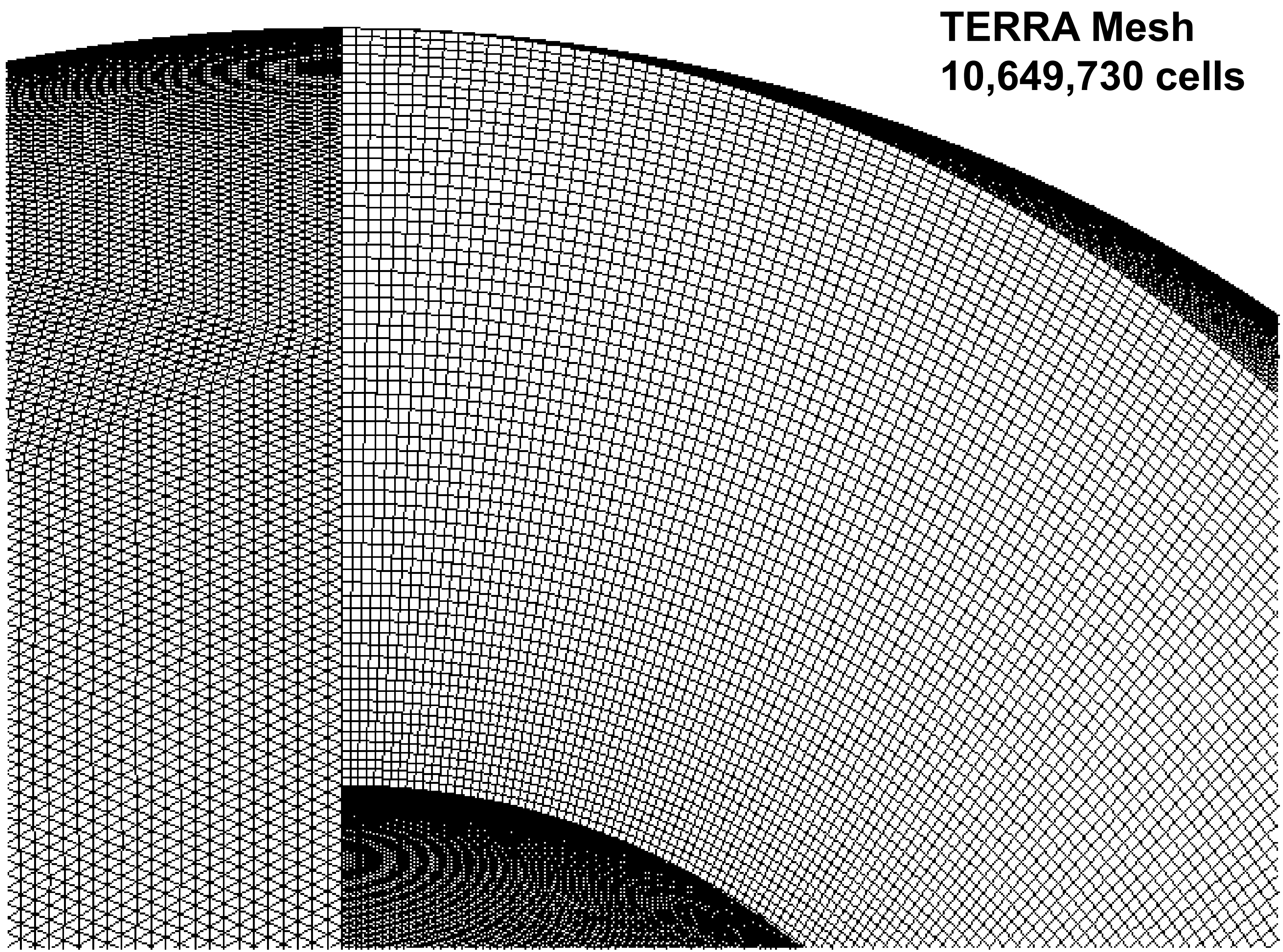
TERRA Mesh
10,649,730 cells

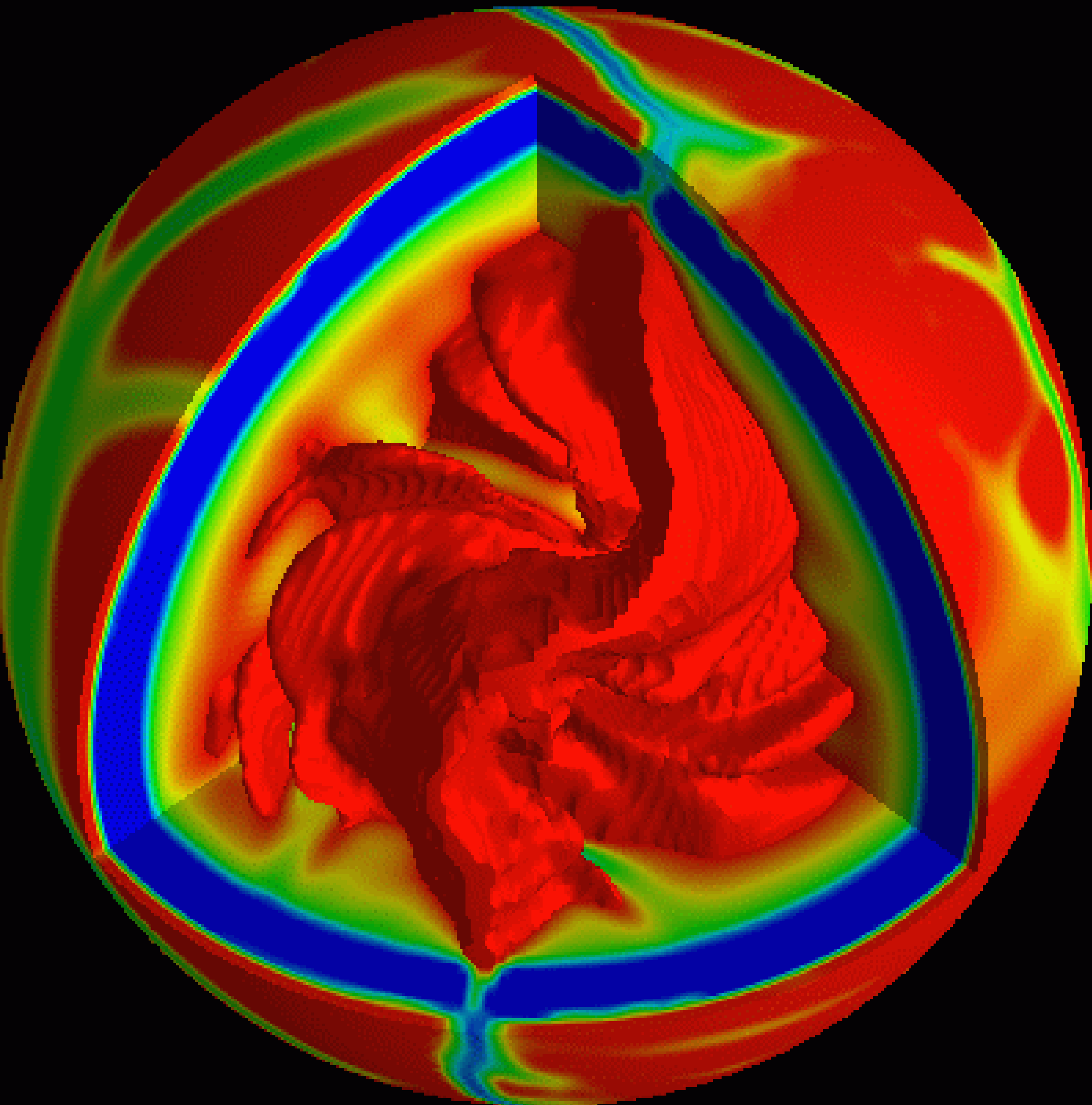

Cutaway view of 3D viscosity field from a case in which high viscosity (red) plate-like patches occur at the outer shell boundary.

This plate-like character appears when a zone of low viscosity (blue) is specified just below the top thermal boundary layer. In the Earth such a zone of reduced viscosity exists in this region almost certainly because of the presence of water.

The contorted red isosurface in the deeper portion of the shell corresponds to the high viscosity cold material sinking from the surface where patches of the upper thermal boundary layer are converging.

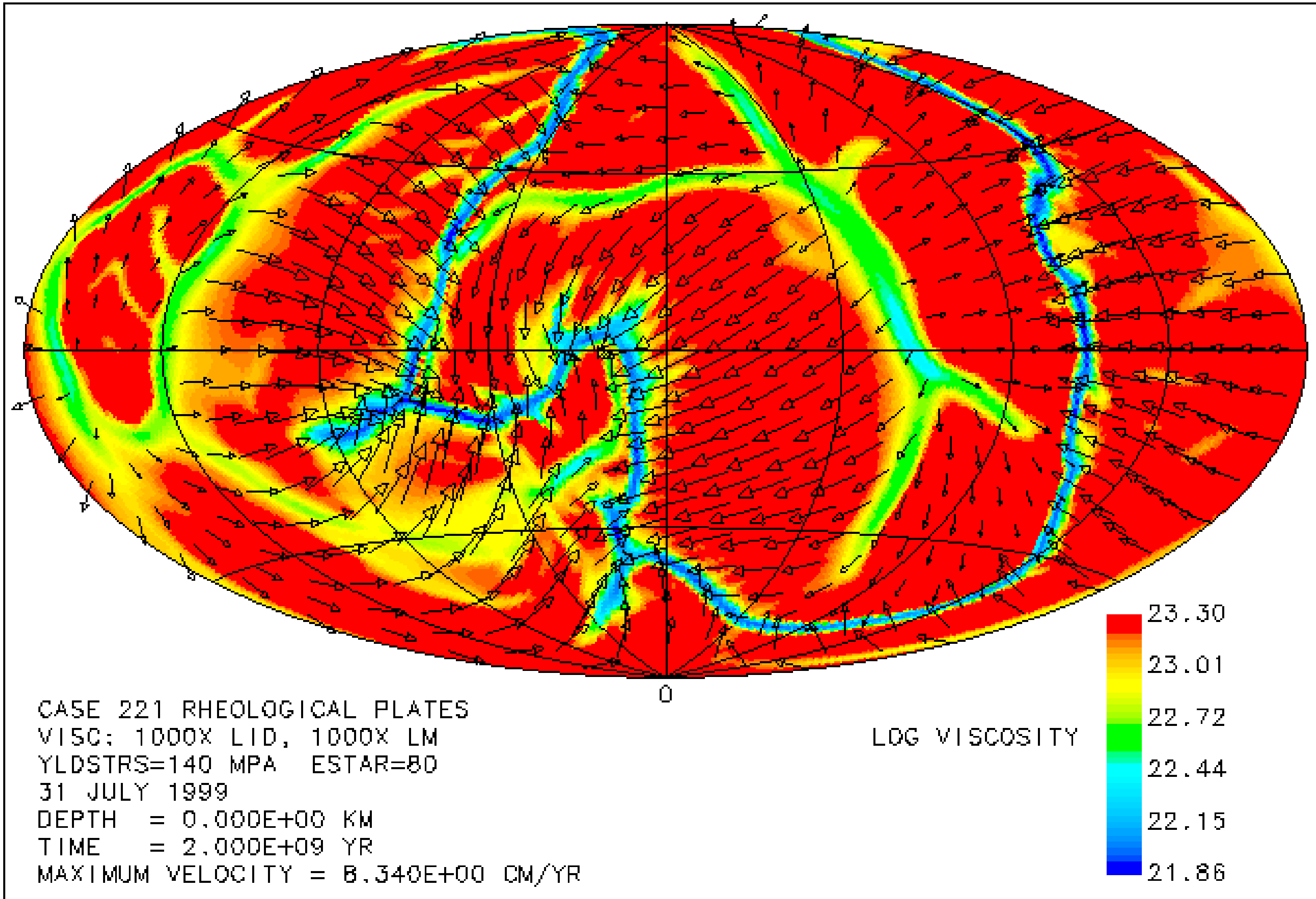
0
CASE 221 RHEOLOGICAL PLATES
VISC; 1000X LID, 1000X LM
YLDSTRS=140 MPA ESTAR=80
31 JULY 1999
DEPTH = 0.000E+00 KM
TIME = 2.000E+09 YR
MAXIMUM VELOCITY = 8.340E+00 CM/YR
LOG VISCOSITY
23.30
23.01
22.72
22.44
22.15
21.86

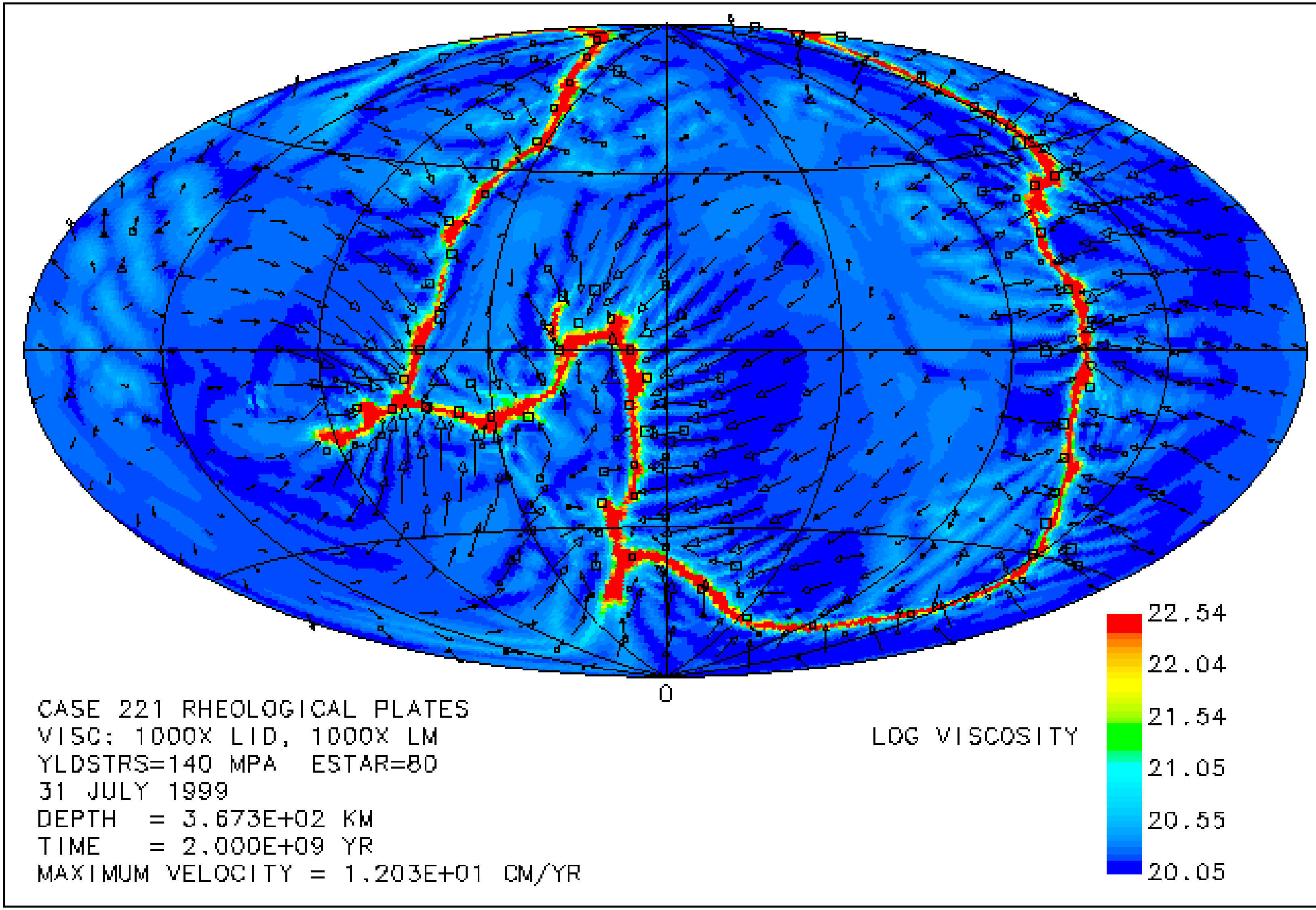
0
CASE 221 RHEOLOGICAL PLATES
VISC: 1000X LID, 1000X LM
YLDSTRS=140 MPA   ESTAR=80
31 JULY 1999
DEPTH = 3.673E+02 KM
TIME = 2.000E+09 YR
MAXIMUM VELOCITY = 1.203E+01 CM/YR
LOG VISCOSITY
22.54
22.04
21.54
21.05
20.55
20.05

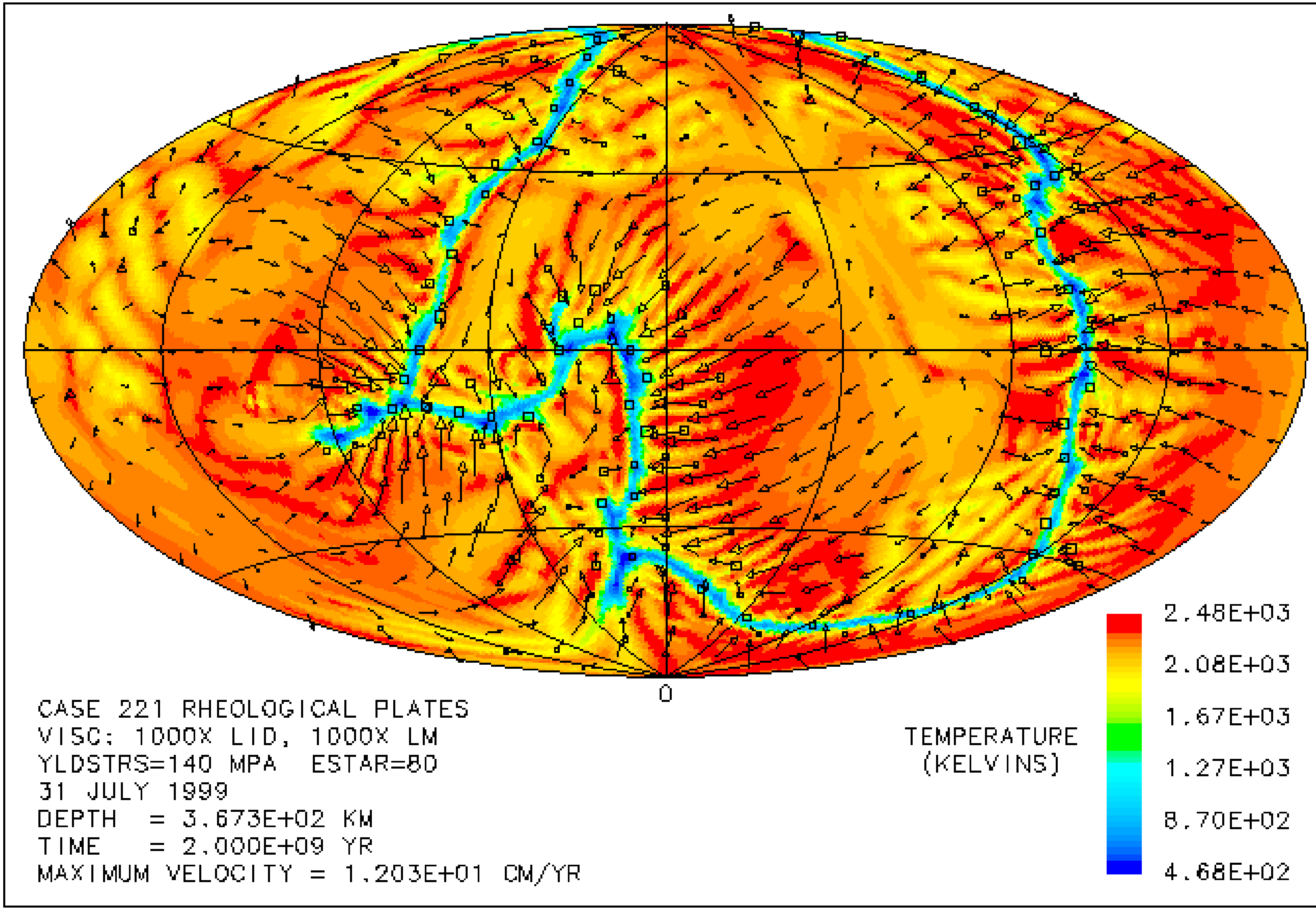
0
CASE 221 RHEOLOGICAL PLATES
VISC: 1000X LID, 1000X LM
YLDSTRS=140 MPA   ESTAR=80
31 JULY 1999
DEPTH   = 3.673E+02 KM
TIME   = 2.000E+09 YR
MAXIMUM VELOCITY = 1.203E+01 CM/YR
TEMPERATURE
(KELVINS)
2.48E+03
2.08E+03
1.67E+03
1.27E+03
8.70E+02
4.68E+02

Lunar Mantle Convection

Stegman, D. R. *et al.* “An early lunar core dynamo driven by thermochemical mantle convection,” *Nature*, *421*, 132-146, 2003.

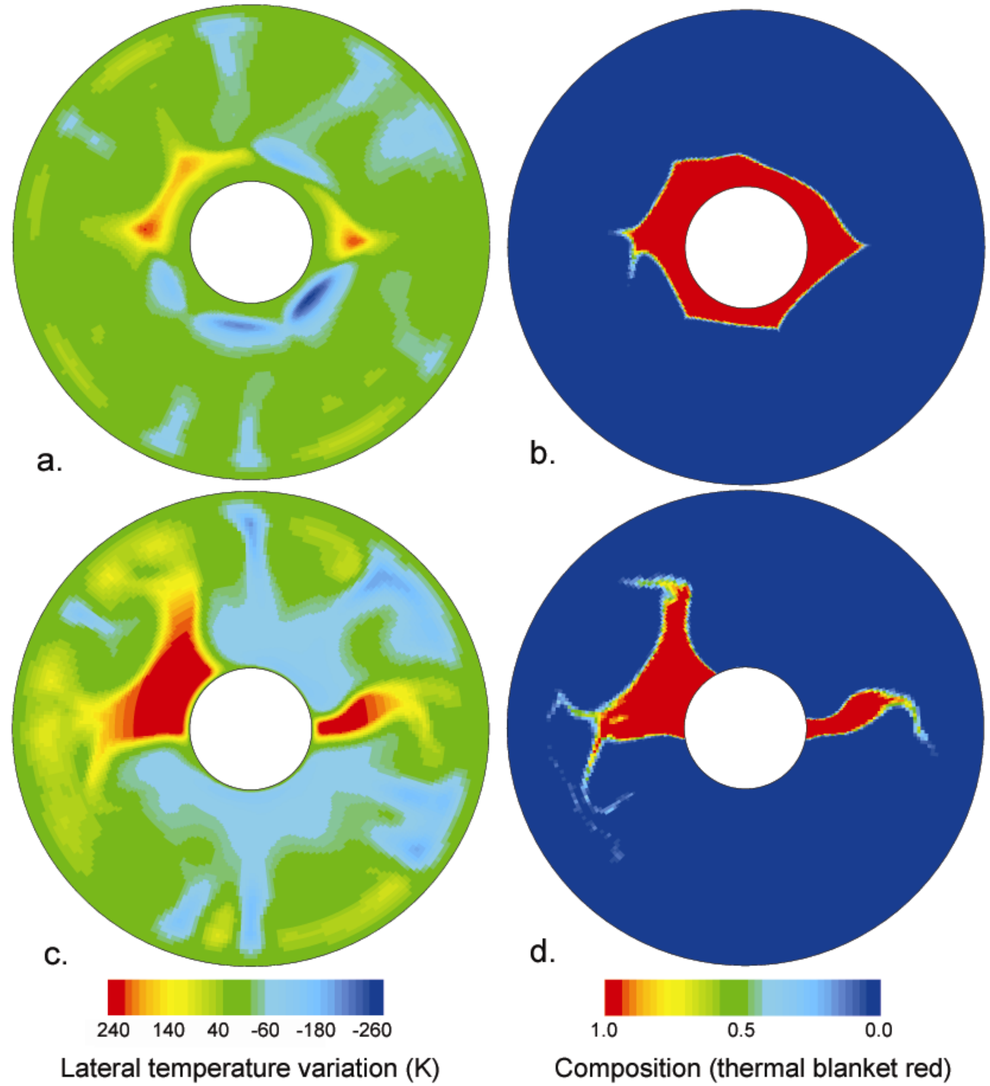

Equatorial cross-sections of temperature and composition for a thermochemical model of lunar history involving a marginally stable ilmenite/KREEP layer 230 km thick initially surrounding the lunar core. Snapshot at 4.3 Ga (a., b.) shows the layer completely enveloping and heating the core. In snapshot at 4.0 Ga (c., d.) the layer has become positively buoyant and is rising in plume-like fashion toward the top of the lunar mantle. The removal of this layer from the core causes a transient core heat flux plausibly high enough to support a short-lived dynamo in the lunar core.

Convection in the Martian Mantle

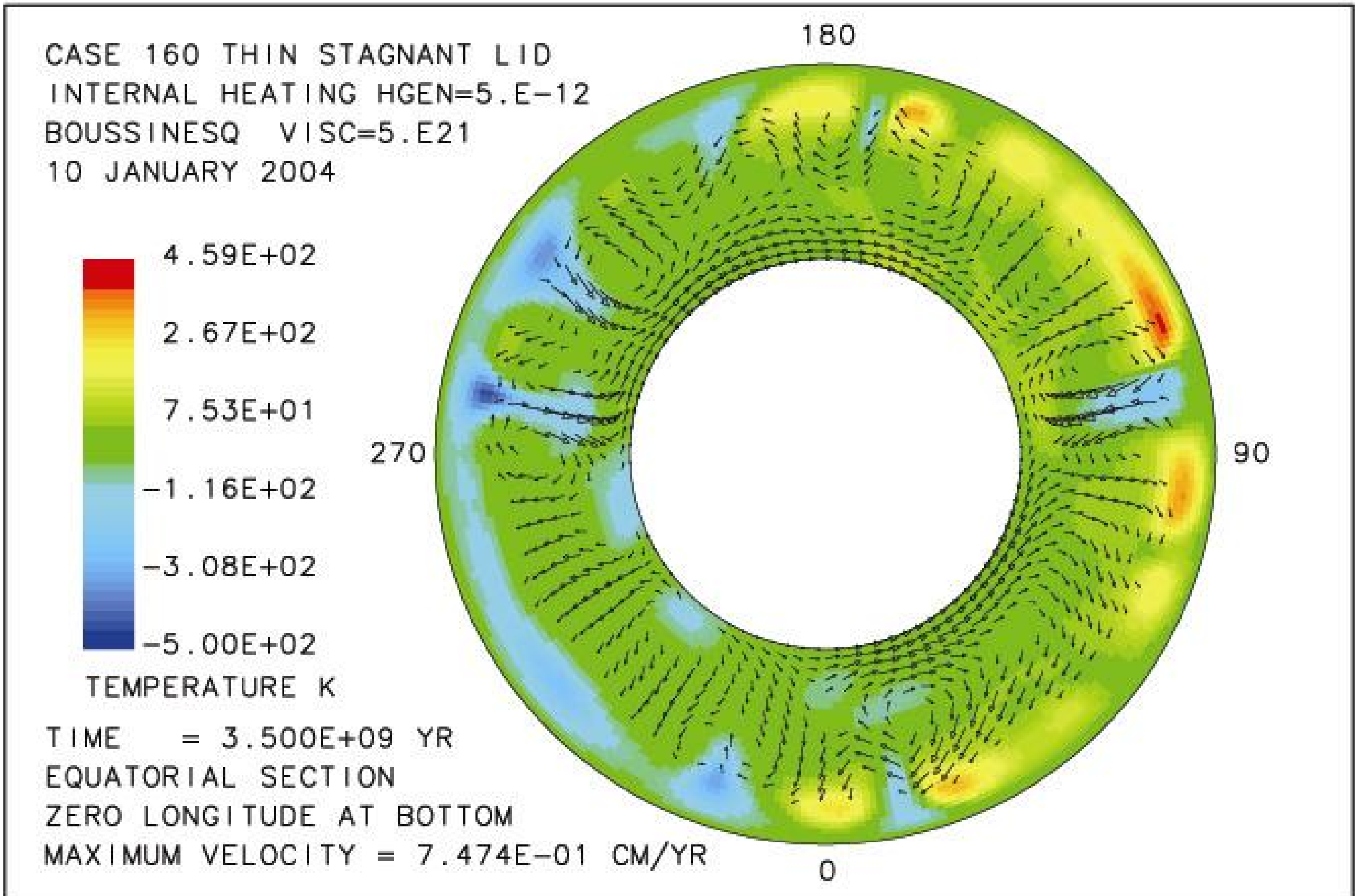

Stagnant lid convection case for Martian mantle.
Color denotes temperature deviation from mean radial value.
Note prominent L=1 component.

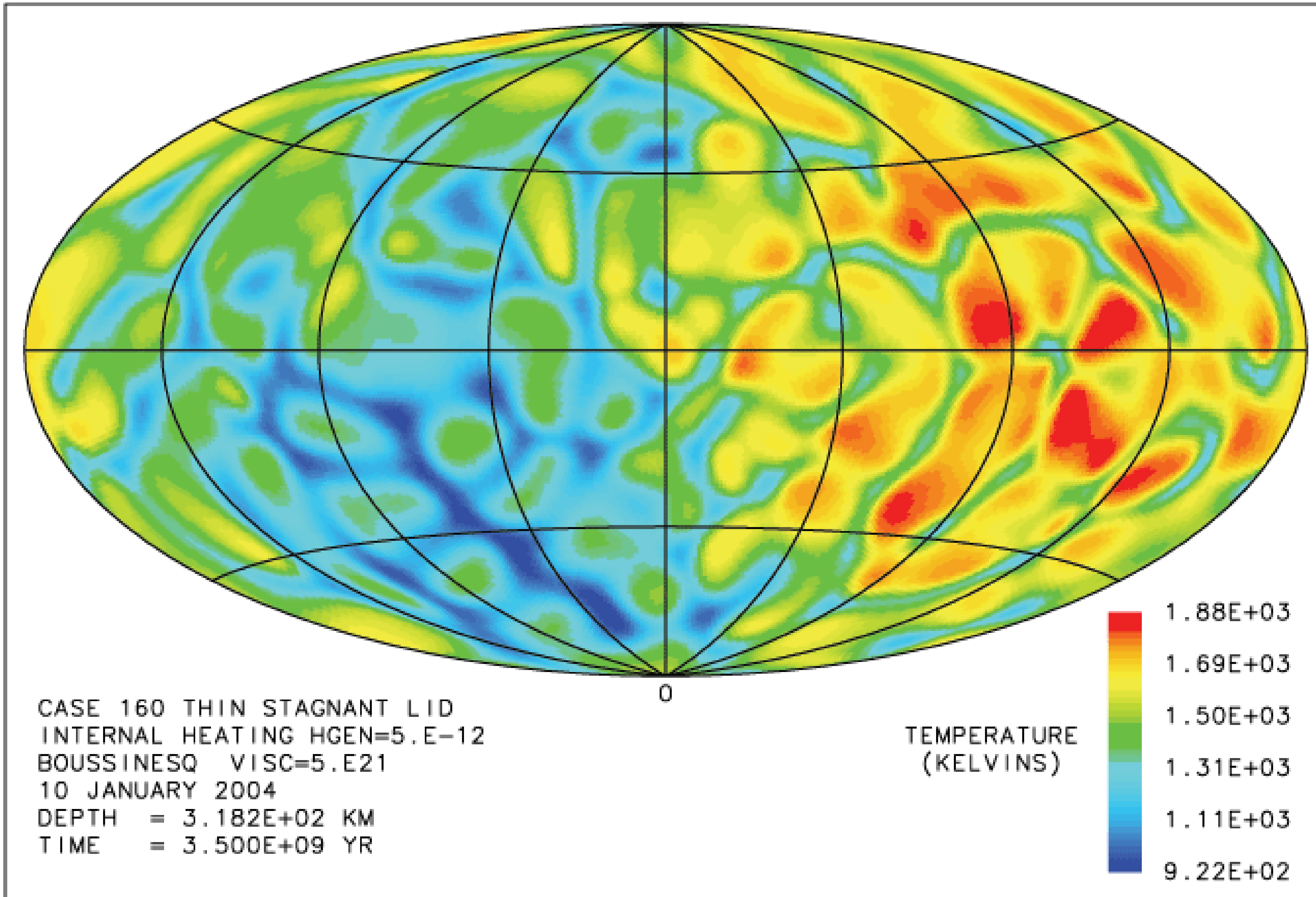

Stagnant lid convection case for Martian mantle.
Color denotes absolute temperature.
Note prominent L=1 component.

Modeling Earth's Plate Tectonic History

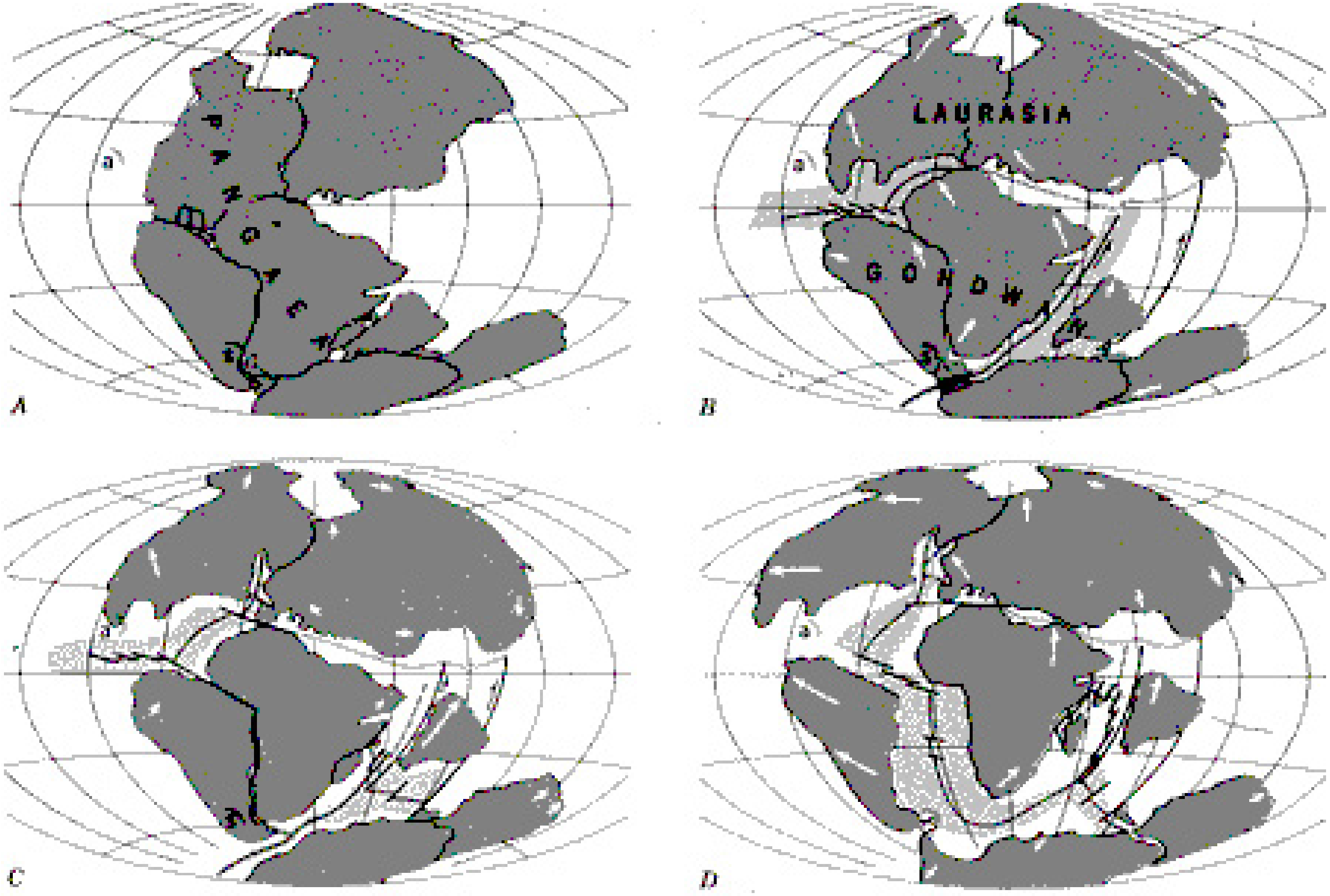

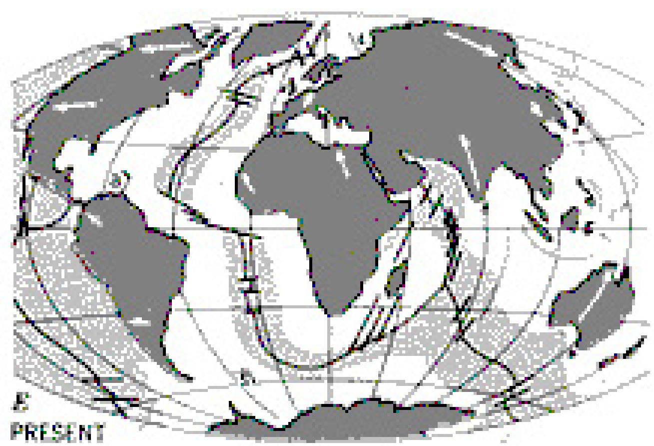

Five snapshots in time of the Earth's continent locations from the time of Pangea to the present.

Approach

- We use a plate treatment that employs passive Lagrangian tracer particles to carry the plate identities. An Euler rotation vector associated with each plate governs the motion of all of the plate's particles.

- The Euler rotation for each plate, in turn, is obtained from the constraint that the integrated torque applied to the volume occupied by that plate vanish.

- The surface velocity field, corresponding to separate uniform rotations for each plate, is then applied as a specified velocity boundary condition.

- A set of simple rules governs the destruction/creation of particles at converging/diverging plate boundaries.

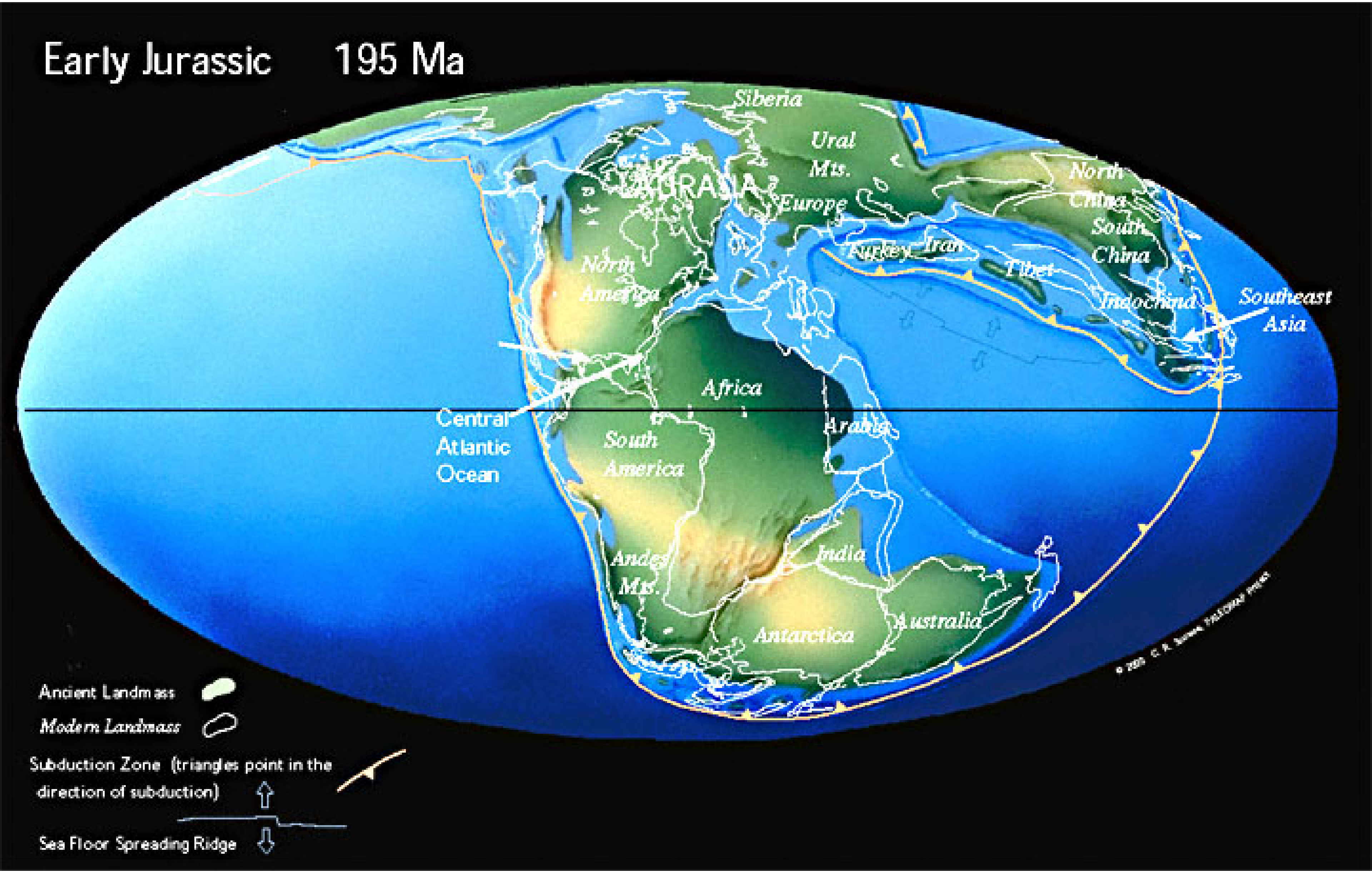
Early Jurassic 195 Ma
Siberia
Ural Mts.
LAURASIA
Europe
North China
South China
Turkey
Iran
Tibet
Indochina
Southeast Asia
North America
Central Atlantic Ocean
Africa
Arabia
South America
Andes Mts.
India
Australia
Antarctica
Ancient Landmass
Modern Landmass
Subduction Zone (triangles point in the direction of subduction)
Sea Floor Spreading Ridge

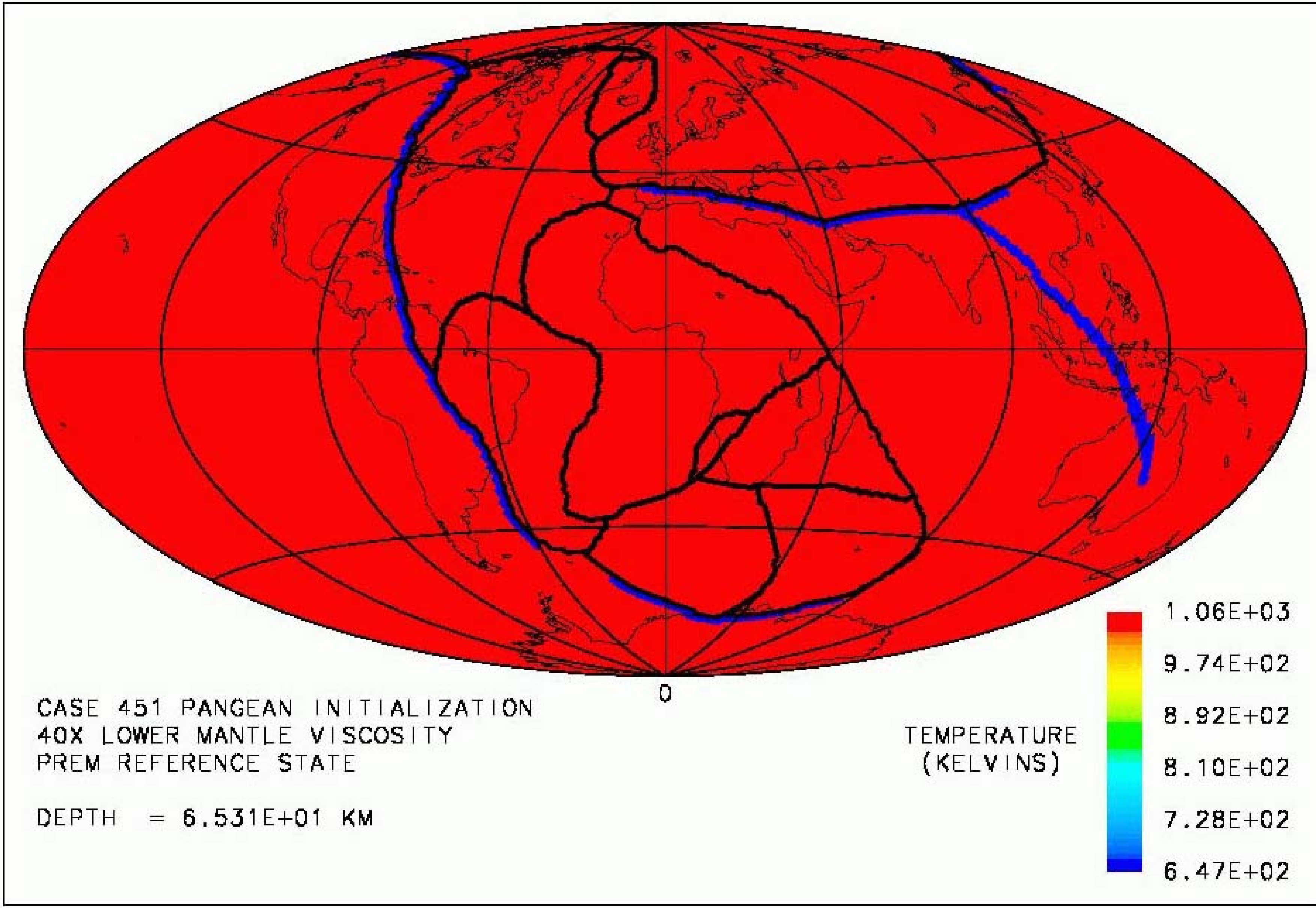

0
CASE 451 PANGEAN INITIALIZATION
40X LOWER MANTLE VISCOSITY
PREM REFERENCE STATE
DEPTH = 6.531E+01 KM
TEMPERATURE
(KELVINS)
1.06E+03
9.74E+02
8.92E+02
8.10E+02
7.28E+02
6.47E+02

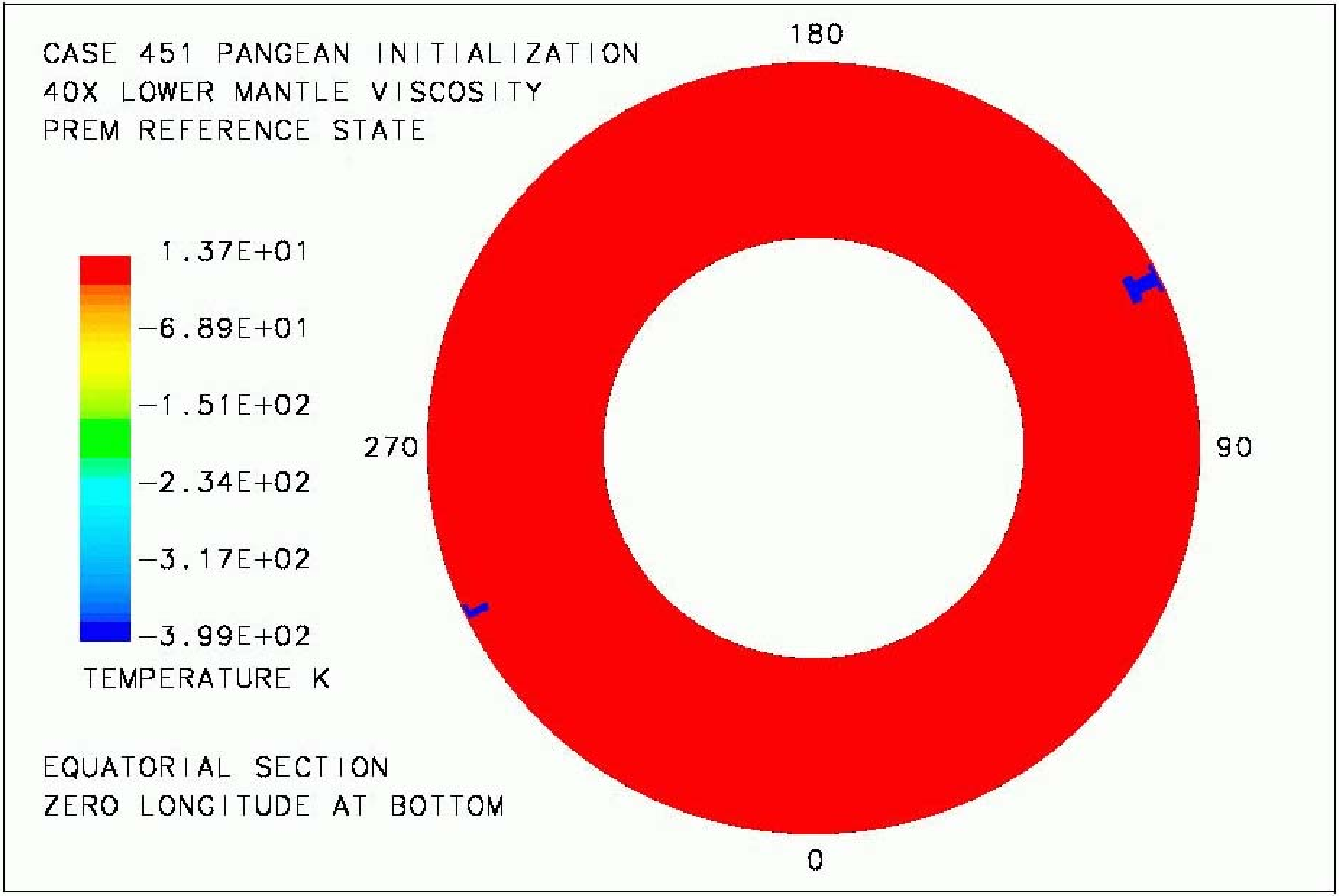
CASE 451 PANGEAN INITIALIZATION
40X LOWER MANTLE VISCOSITY
PREM REFERENCE STATE
180
270
90
0
1.37E+01
-6.89E+01
-1.51E+02
-2.34E+02
-3.17E+02
-3.99E+02
TEMPERATURE K
EQUATORIAL SECTION
ZERO LONGITUDE AT BOTTOM

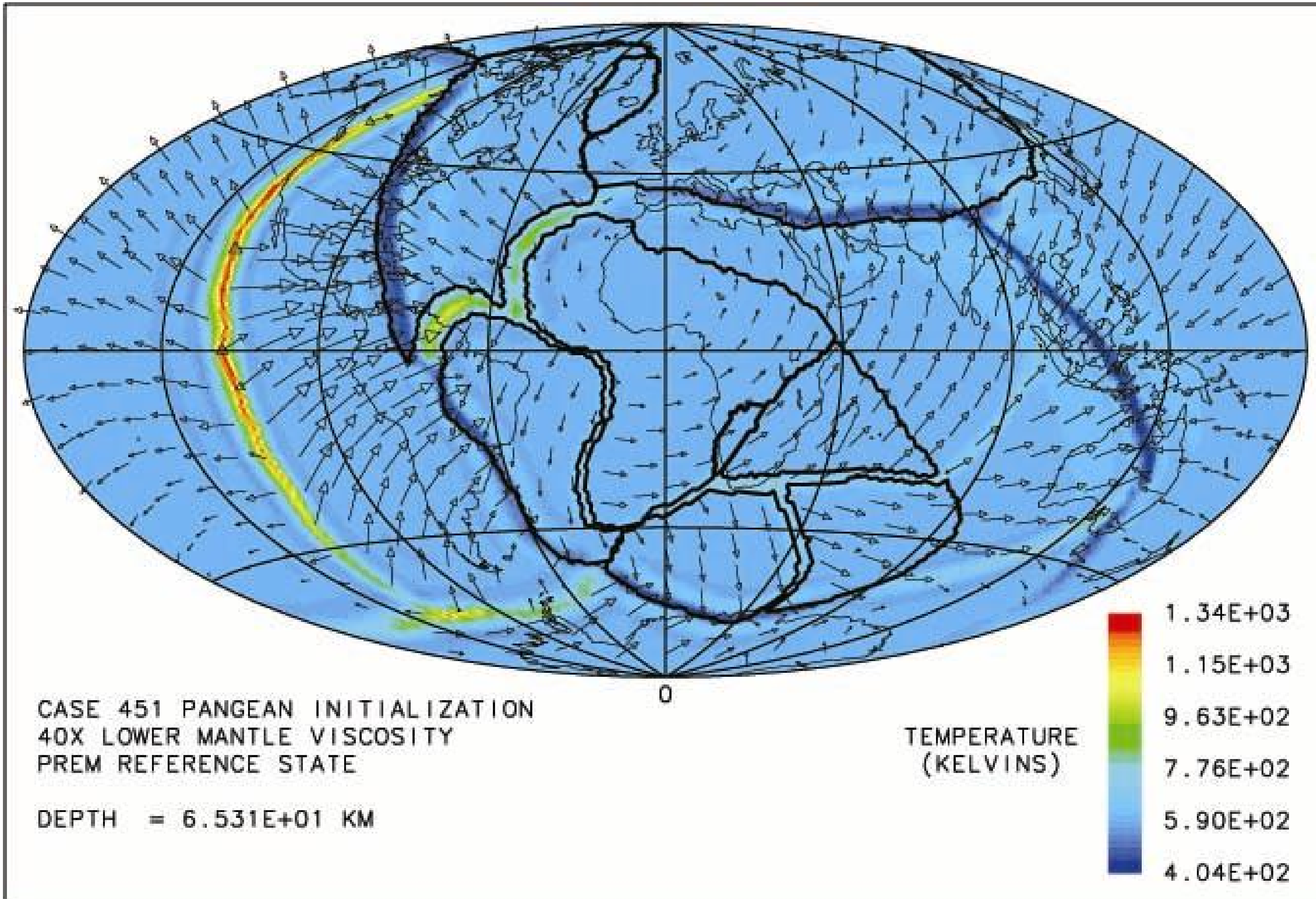
0
CASE 451 PANGEAN INITIALIZATION
40X LOWER MANTLE VISCOSITY
PREM REFERENCE STATE
DEPTH = 6.531E+01 KM
TEMPERATURE
(KELVINS)
1.34E+03
1.15E+03
9.63E+02
7.76E+02
5.90E+02
4.04E+02

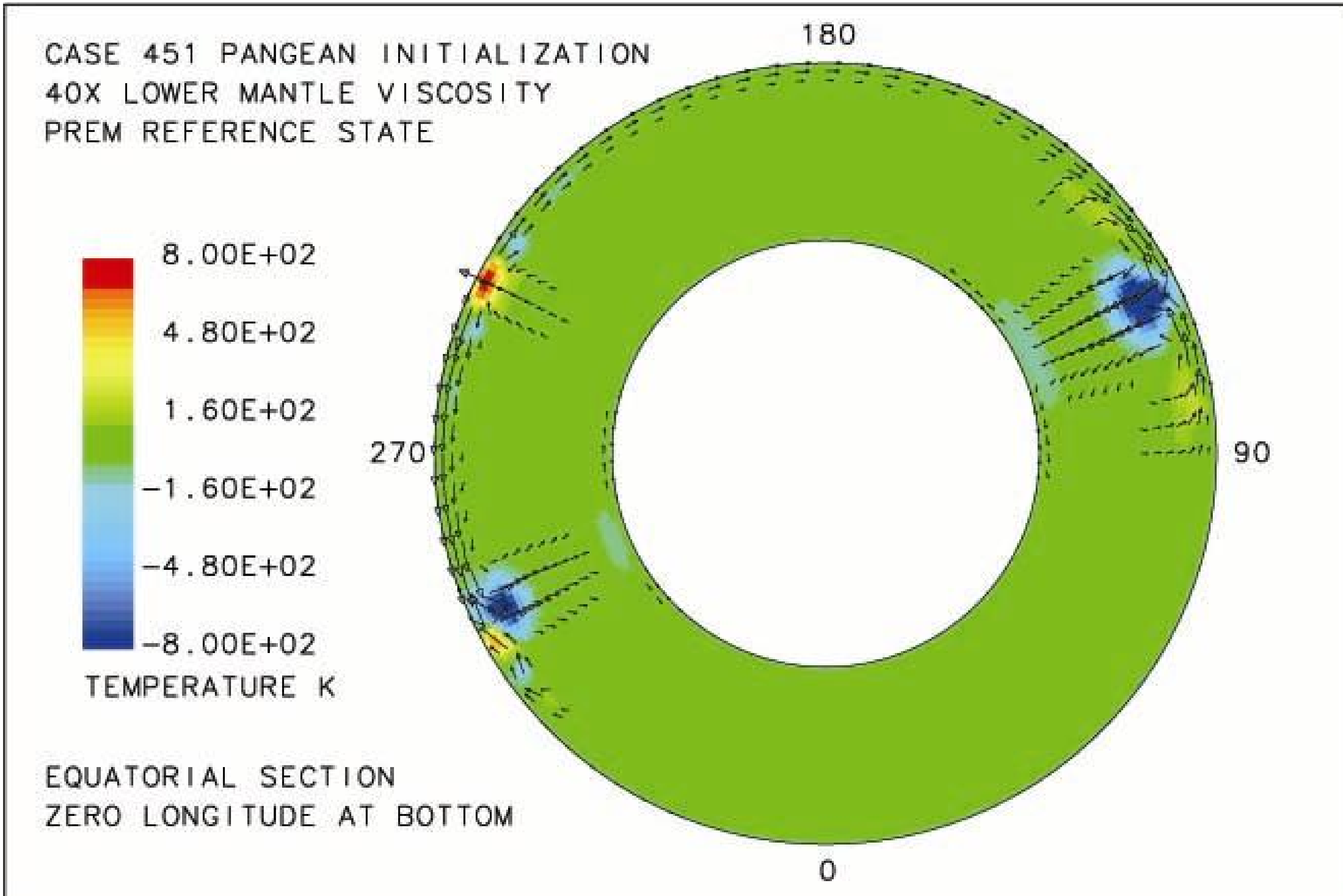
CASE 451 PANGEAN INITIALIZATION
40X LOWER MANTLE VISCOSITY
PREM REFERENCE STATE
8.00E+02
4.80E+02
1.60E+02
-1.60E+02
-4.80E+02
-8.00E+02
TEMPERATURE K
EQUATORIAL SECTION
ZERO LONGITUDE AT BOTTOM
180
270
90
0

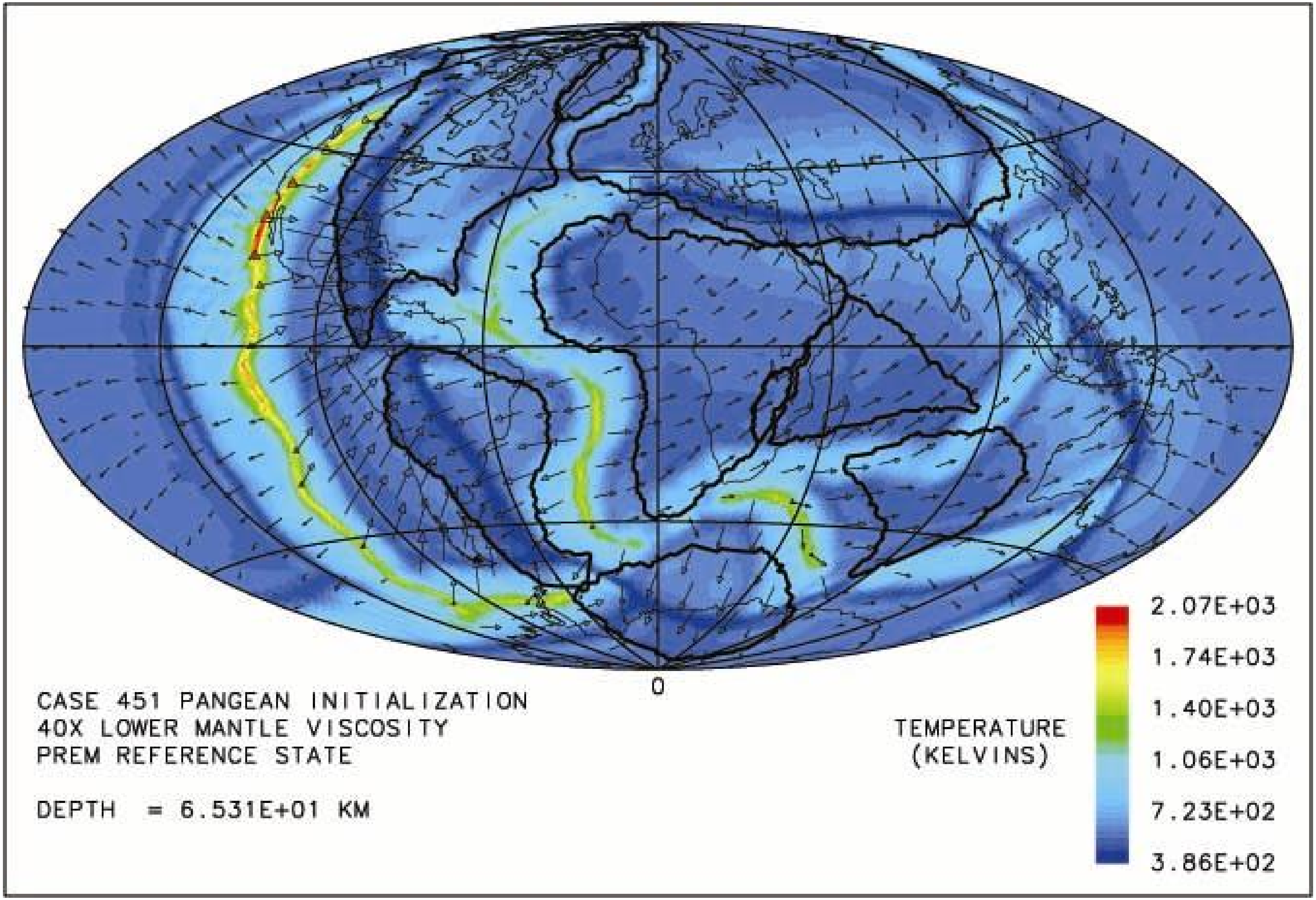
0
CASE 451 PANGEAN INITIALIZATION
40X LOWER MANTLE VISCOSITY
PREM REFERENCE STATE
DEPTH = 6.531E+01 KM
TEMPERATURE
(KELVINS)
2.07E+03
1.74E+03
1.40E+03
1.06E+03
7.23E+02
3.86E+02

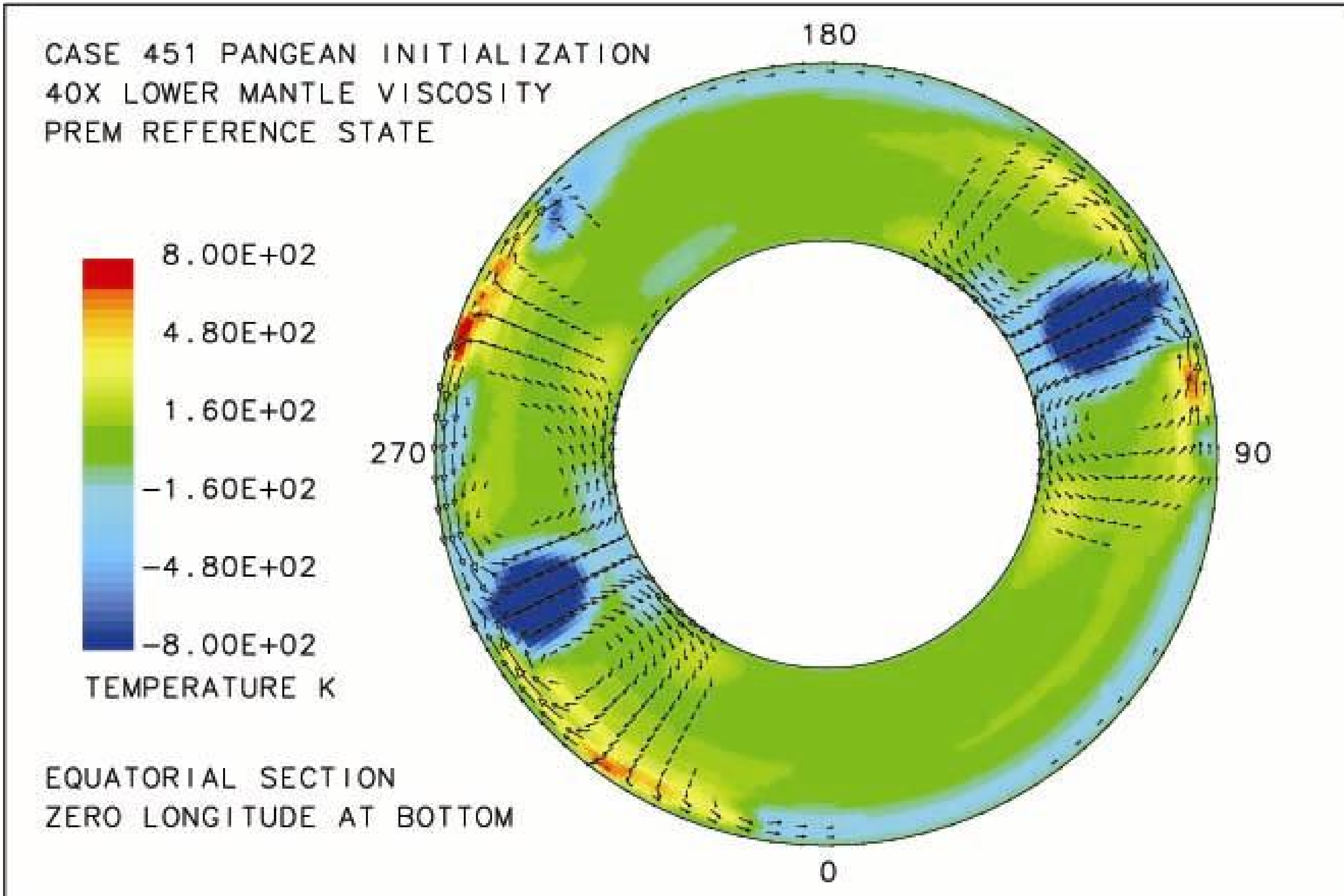

CASE 451 PANGEAN INITIALIZATION
40X LOWER MANTLE VISCOSITY
PREM REFERENCE STATE
8.00E+02
4.80E+02
1.60E+02
-1.60E+02
-4.80E+02
-8.00E+02
TEMPERATURE K
EQUATORIAL SECTION
ZERO LONGITUDE AT BOTTOM
180
270
90
0

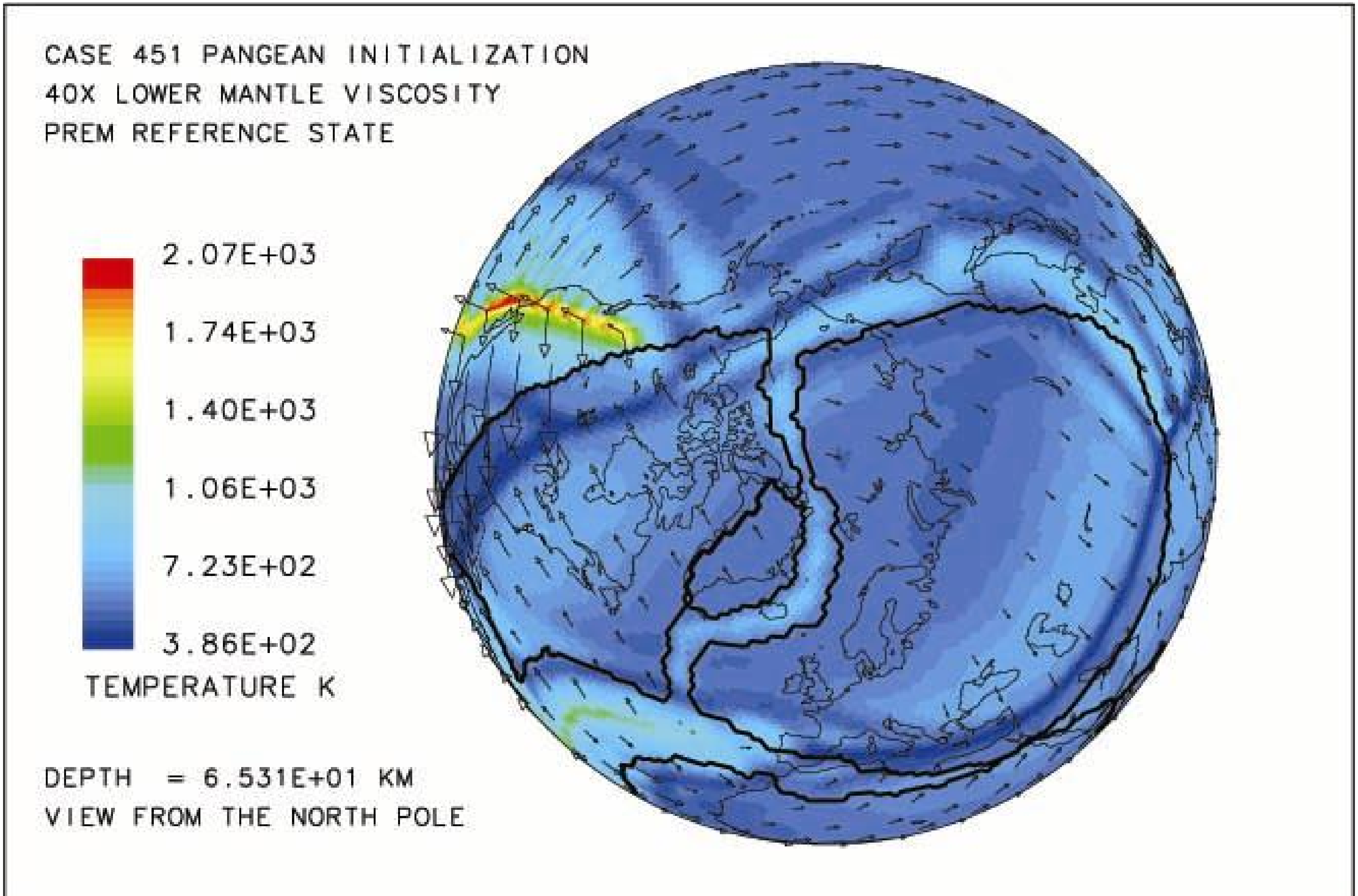
CASE 451 PANGEAN INITIALIZATION
40X LOWER MANTLE VISCOSITY
PREM REFERENCE STATE
2.07E+03
1.74E+03
1.40E+03
1.06E+03
7.23E+02
3.86E+02
TEMPERATURE K
DEPTH = 6.531E+01 KM
VIEW FROM THE NORTH POLE

Benchmarking 3D Codes

Analytical benchmark:

Surface deformations, geoid, pressure and velocity fields resulting from single spherical harmonic density perturbation at a specified radial position in the spherical shell.

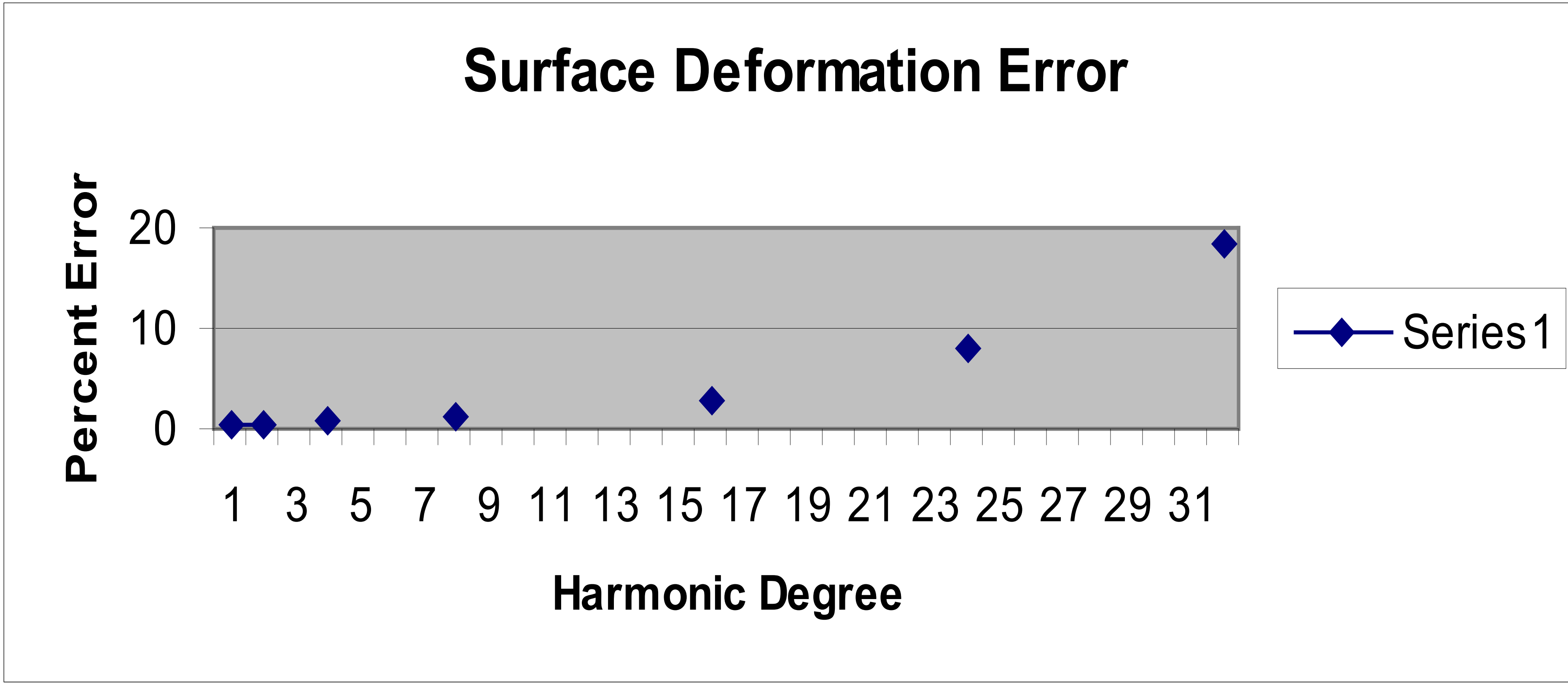

Surface Deformation Error
Percent Error
20
10
0
1 3 5 7 9 11 13 15 17 19 21 23 25 27 29 31
Harmonic Degree
Series1